

# **Integration of alumina ultrafiltration membrane and palladium-catalyzed peroxymonosulfate for removal of organic micropollutants**

He Tian 5606748

In partial fulfillment of the requirements for the degree of

**Master of Science**

In Civil Engineering

at the Delft University of Technology.

Assessment committee:	Dr. Ir. S.G.J Heijmen (Chair)
	Prof. Dr. Ir. L.C. Rietveld
	Prof. Dr. Ir. Henri Spanjers
	Dr. Ir. Begum Tanis
Daily supervisor	Ir. Shuo Zhang

## Abstract

Organic micropollutants (OMPs) originate from organic chemicals such as drugs and pesticides that are widely used in human activities. OMPs are difficult to remove by conventional water treatment techniques, and hence continue to accumulate in natural water bodies. More effective methods need to be investigated for the removal of OMPs in drinking water treatment because of their toxicity and carcinogenicity, which may pose potential risks to human health. Previous studies have suggested that the use of activated peroxymonosulfate (PMS) catalyzed by Palladium (Pd) immobilized in ultrafiltration (UF) membranes can effectively degrade 1,4-dioxane and p-nitrophenol, while its removal efficiency for other OMPs, limiting factors and reaction mechanism still require for more research. In this study, PMS-Pd/UF system was established by coating Pd on the surface and 20 nm pores of the ultrafiltration membrane. The effectiveness of PMS-Pd/UF in the removal of OMPs from ultrapure water under various flux, pH, PMS dosages and ions presence was examined, as well as the performance in other water matrices including simulated brackish water, simulated brine water and river water. The results showed that PMS-Pd/UF achieved more than 95% of OMPs removal in 1 and 12-hour filtration tests at a flux of 30 LMH, while removal efficiency decreased with the increased flux due to the reduced contact time. The pH tests indicated that the system was more efficient under a neutral pH environment. The presence of 1 mM of various ions ( $\text{Cl}^-$ ,  $\text{HCO}_3^-$ ,  $\text{SO}_4^{2-}$ , and  $\text{ClO}^-$ ) had limited effects on the degradation of OMPs. However, the removal of OMPs was inhibited when OMPs coexisted with NOM in river water and, in combination with high salt concentrations simulated brine water (e.g., with 250mM of total anions). From specific scavenger dosing experiments, it was concluded that  $\text{SO}_4^{\bullet-}$ ,  $\bullet\text{OH}$ , and  $\text{O}_2^{\bullet-}$  were the main reactive species induced from Pd/UF-activated PMS for the removal of OMPs.

# Content

Abstract .....	I
Abbreviation list .....	III
1 Introduction .....	1
1.1 Background .....	1
1.2 Research objective and questions .....	3
2 Literature review .....	4
2.1 Organic micropollutants .....	4
2.2 Membrane filtration.....	4
2.3 Advanced oxidation processes .....	7
2.4 Integration of AOP and UF membranes .....	12
3 Methodology .....	15
3.1 Chemicals and reagents .....	15
3.2 Ultrafiltration membrane information .....	15
3.3 ALD-Pd method .....	16
3.4 OMPs removal experiments .....	17
3.5 Reactive species determination experiments.....	19
3.6 Surface Pd and pores Pd determination experiments .....	20
4 Results and discussions .....	22
4.1 OMPs degradation by Pd/UF activated PMS .....	22
4.2 Determination of the functional reactive species.....	27
4.3 Role of Pd coated on the surface and in the pores.....	30
5 Limitations and recommendations .....	31
6 Conclusion.....	33
7 Reference.....	34
8 Appendix .....	42

## Abbreviation list

Abbreviation	Definition
AA	L-ascorbic acid
ALD	Atomic layer deposition
AOPs	Advanced oxidation processes
BT	Benzothiazole
CA	Cellulose acetate
CBZ	Carbamazepine
COD	Chemical oxygen demand
CVD	Chemical vapor deposition
DIC	Diclofenac
FFA	Furfuryl alcohol
HR-AOPs	Hydroxyls radical-based advanced oxidation processes
MF	Microfiltration
MP	Metoprolol
MWCO	Molecular weight cut-off
NF	Nanofiltration
NOM	Natural organic matter
OMPs	Organic micropollutants
PDS	Peroxydisulfate
PMS	Peroxymonosulfate
PP	Polypropylene
PPL	Propranolol
RO	Reverse osmosis
ROS	Reactive oxygen species
RS	Reactive species
SOT	Sotalol
SR-AOPs	Sulfate radical-based advanced oxidation processes
TBA	Tert-butanol
TMP	Transmembrane pressure
TMP	Trimethoprim
TOC	Total organic carbon
UF	Ultrafiltration

# 1 Introduction

## 1.1 Background

Organic micropollutants (OMPs), such as pharmaceuticals, pesticides, personal care products, and endocrine disrupting chemicals, are frequently released into the aquatic environment through the wastewater treatment system [1]. Although their concentrations in nature are generally ng/L to low  $\mu\text{g/L}$ , their long-term exposure to water bodies can have negative impacts on ecosystems and human health due to their toxicity, persistence and bioaccumulation potential [2]. Furthermore, because of the increasing demand for chemicals, the levels of OMPs in natural water bodies will continue to increase. Therefore, removing OMPs from source water is a severe challenge for current water treatment plants to ensure water security.

Membrane technology is widely used in water treatment because it is more compact and effective than traditional water treatment technologies in removing contaminants from water. Studies have shown that nanofiltration (NF) and reverse osmosis (RO) can completely or nearly remove a wide variety of OMPs from water [3]. However, one of the drawbacks of RO and NF is that biopolymers and other NOMs can accumulate in the membrane modules causing membrane fouling and reducing treatment efficiency. Also, the concentrated OMPs streams from membrane filtration are difficult to be handled except by direct discharge to the natural environment or requirement of further advanced treatment. Previous studies have revealed that combining catalytic membranes with the advanced oxidation processes (AOPs) could enhance the removal of OMPs in a single stage, and mitigate the risk of concentrated streams produced from the conventional technology. Although ultrafiltration (UF) membranes cannot reject OMPs due to their relatively larger pore sizes (10 – 100 nm) [4], it is possible to immobilize catalysts within their nanoscale pores. The efficiency of AOPs is sometimes compromised due to rapid self-quenching of short lifetime reactive species. However, the pores of UF can confine the reactive species and OMPs within the nanoscale, which greatly enhances the possibility for them to approach and react with each other, and hence the effectiveness, selectivity, and reactivity of the reactive species are greatly enhanced [5,6]. In terms of material selection for catalytic membranes, studies in the last decades have highlighted the advantages of ceramic membranes over their polymer counterparts. For example, ceramic membranes made of materials like  $\text{Al}_2\text{O}_3$  or  $\text{TiO}_2$  have a higher thermal stability, which contributes to their extended lifespan [7]. Additionally, these membranes can withstand strong acid and alkali corrosion, making them more durable in harsh operating conditions [8].

AOPs have a greater ability to degrade organic matter than normal oxidation processes because

they produce reactive species with greater oxidizing capacity as secondary oxidants, thus they are widely used in the water treatment [9]. Depending on the method, AOP can be activated by chemical, physical, photochemical, photocatalytic, and electrochemical processes. All of them aim to produce strong oxidizing reactive species to decompose organic pollutants [10]. Fenton reaction, one of the hydroxyls radical-based AOPs (HR-AOPs) technologies, is widely used to degrade the OMPs. However, due to the moderate reduction potential of 1.7 - 2.5 V for the  $\cdot\text{OH}$  radicals induced by the Fenton reaction, researchers turned to the search for more efficient AOP methods [11].

Peroxymonosulfate (PMS,  $\text{HSO}_5^-$ ) was introduced as a new chemical oxidizer for the degradation of OMPs. The  $\text{HSO}_5^-$  ion is a derivate of  $\text{H}_2\text{O}_2$  in which one H-atom is replaced by a  $\text{SO}_3^-$  group [12]. It has an oxidation potential similar to that of  $\text{H}_2\text{O}_2$  (1.8V), so it is able to slowly oxidize some organic substances. However, the oxidation ability of PMS can be promoted by catalysis, the activated-PMS produces both  $\cdot\text{OH}$  and  $\text{SO}_4^{\cdot-}$  (Sulfate radical).  $\text{SO}_4^{\cdot-}$  is a stronger one-electron oxidant with an oxidation potential of 2.5 - 3.1V, which indicates it can degrade organic matter more effectively than  $\cdot\text{OH}$  [13]. In addition,  $\text{SO}_4^{\cdot-}$  works on a broader pH range (pH 3-9) than  $\cdot\text{OH}$  (pH < 4.0) [13,14]. Except for  $\cdot\text{OH}$  and  $\text{SO}_4^{\cdot-}$ , superoxide radicals ( $\text{O}_2^{\cdot-}$ ), singlet oxygen ( $^1\text{O}_2$ ) were also found in the activated-PMS system, which also contributed to the degradation of OMPs [15].

PMS can be activated by various methods, including thermal, UV, metal or metal oxide, but their mechanisms are all based on breaking the peroxide bond of the PMS [16]. In the context of metal and metal oxide activation, cobalt ions ( $\text{Co}^{2+}$ ) have demonstrated the highest efficacy in activating PMS among all transition metals [17]. However, the potentially carcinogenic property of  $\text{Co}^{2+}$  and its oxides hampers its application in water treatment [18]. As a result, researchers have decided to explore alternative activators, including noble metals like palladium (Pd), platinum (Pt), gold (Au), and silver (Ag), which have attracted more attention due to their remarkable ability to induce PMS to generate reactive species [13]. It was shown that among these noble metals, Pd exhibited the strongest ability to activate PMS for degradation of OMPs [13]. Subsequent experiments have revealed that Pd-activated PMS can more efficiently oxidize OMPs compared to the conventional Fenton reaction [14].

Atomic layer deposition (ALD) is one of the chemical surface coating techniques. ALD's cyclic and self-saturating nature gives it conformality and control over coating thickness and composition [19]. Studies have successfully used the ALD method to immobilize various transition metals and noble metals on the  $\text{Al}_2\text{O}_3$ ,  $\text{SiO}_2$ , and  $\text{TiO}_2$  surface. Lu et al. were the first to use ALD to load Pd nanoparticles on  $\text{Al}_2\text{O}_3$ -based ceramic membranes, and the synthesized catalytic membrane exhibited improved oxidation ability for p-nitrophenol [20]. Feng et al.,

compared the efficiency of Pd/Al<sub>2</sub>O<sub>3</sub> - PMS with other common oxidants, including H<sub>2</sub>O<sub>2</sub>, PDS and copper-iron bimetallic activator for the degradation of 1,4-dioxane, and the results demonstrated that the highest degradation efficiency was achieved by using Pd-activated PMS [14].

However, the removal efficiency of the system for a wider range of OMPs species is currently unknown. Therefore, in this study, 7 common pharmaceuticals were selected from the 11 target OMPs for wastewater treatment listed by the Dutch Ministry of Infrastructure and Water Management as pollutants to examine the performance of PMS-Pd/UF [21]. In addition, current research leaves gaps in understanding how to improve its performance and what the limiting factors are during the process. Also, the performance of PMS-Pd/UF in natural water bodies, such as brackish and surface water, has not been examined. Therefore, in order to comprehensively evaluate the ability of PMS-Pd/UF in removing OMPs, the effects of different flux, pH, PMS dosage and natural water constituents on the system performance need to be investigated. Moreover, some studies reported that besides for  $\cdot\text{OH}$  and  $\text{SO}_4^{\cdot-}$ ,  $^1\text{O}_2$  and  $\text{O}_2^{\cdot-}$  were also found in the PMS-Pd/UF system, which might contribute to the oxidation of some OMPs. Therefore, the mechanism of OMPs degradation by PMS-Pd/UF also needs to be verified using quenching experiments.

In this study, Pd was deposited on the surface/into the pore of the 20 nm UF membranes via ALD method with 60 cycles, forming a 1.20 nm Pd layer. The 20 nm UF is selected because it has been reported that a pore size less than 25 nm would enhance the degradation of OMPs owing to the effect of nano confinement [22]. In order to verify the promoting effect of nano confinement on the system performance, this experiment also compares the efficiency of Pd on the surface and Pd in the pores to catalyze PMS for the removal of OMPs.

## 1.2 Research objective and questions

This research aims to assess the combination of ALD-modified catalytic membrane with AOP in water treatment.

The followings are the research questions to achieve the objective:

1. What is the impact of factors, such as flux, pH, ions, PMS concentrations on the degradation efficiency of OMPs?
2. What is the main reactive species that plays the dominant role in the oxidation of OMPs by Pd-catalyzed PMS?
3. What are the effects of the catalyst on the surface and in the pores on the PMS-Pd/UF system performance?

## 2 Literature review

### 2.1 Organic micropollutants

OMPs can enter natural waterbodies and contaminate drinking water sources by various pathways including industrial processes, and agricultural activities. In addition, the extensive use of pesticides, pharmaceuticals, cosmetics and other organic products are also major contributors of OMPs to the environment [23]. OMPs are of concern because they can adversely affect water quality, ecosystems, and human health at very low concentrations (from ng/L to low µg/L) [2]. OMPs in the natural waterbodies can cause chronic effects on aquatic organisms, including endocrine disruption and antibiotic resistance [24]. Besides, they can adsorb toxic compounds and heavy metals, which can accumulate in aquatic organisms after ingestion and are potentially toxic to them [25]. OMPs can also enter human bodies through contaminated drinking water and food chain. Studies have shown that the long-term exposure to OMPs has been associated with increased risk of diabetes, obesity, endocrine disruption, cancer, and reproductive disorders among humans [26]. Therefore, it is essential for drinking water plants to implement appropriate treatment strategies and advanced technologies to effectively remove OMPs, in order to ensure the safety of the drinking water supply.

The technologies applied to remove OMPs in drinking water treatment can be summarized into three main categories, namely adsorption, advanced oxidation processes and membrane filtration [27]. In this sector, advanced oxidation processes and membrane filtration are introduced.

### 2.2 Membrane filtration

Membrane filtration is a physical separation technique, using a membrane to mechanically sift solutes, colloids, or fine particulate from solutions. Membrane filtration can be divided into four types based on their pore sizes as shown in [Figure 1](#): 1). Microfiltration (MF) which has the largest pore size in the range of 0.1 – 10 µm and is mainly used to remove suspended solids and bacteria from water. 2). Ultrafiltration membrane (UF) has a pore size range of 10 to 100 nm, which can effective rejection of particles such as colloids and proteins. 3). Nanofiltration (NF) has the ability to separate multivalent ions, dissolved organics and virus ranged from 1 – 10 nm. 4). Reverse osmosis (RO) is the finest membrane with pores smaller than 1 nm and can effectively reject monovalent ions.

#### 2.2.1 Rejection mechanism

The basic mechanism of membranes to reject OMPs is size exclusion. Both RO and NF can

rejecting OMPs, RO membranes has a molecular weight cut-off (MWCO) below 200 Da and NF membranes with pore sizes around 1 nm and a MWCO ranging from 200 to 1000 [27]. This is because the majority of OMPs have a molecular size of approximately 0.8 nm and a molecular weight falling between 200 and 300 g/mol [28]. In addition to the size exclusion, electrostatic repulsion and solute-membrane interactions are also important mechanisms for the removal of OMPs by membrane filtration, especially when the size of the OMPs is smaller than the MWCO of membranes.

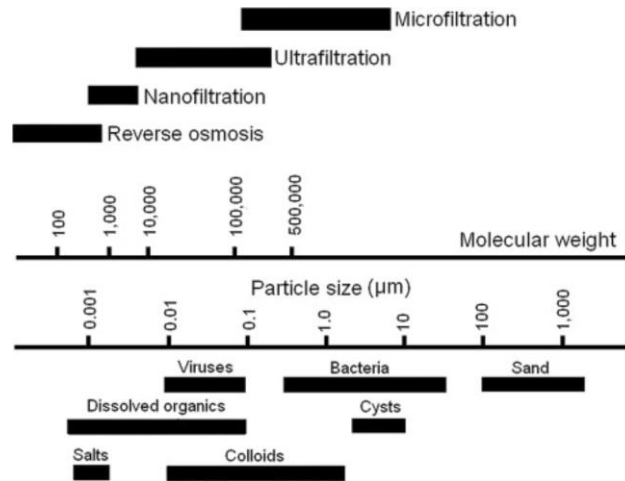


**Figure 1: Particle removal ranges for membrane systems** 错误!未找到引用源。

Electrostatic repulsion's impact is based on the characteristics of the solution, membranes, and OMPs. The charge present on the membranes and the OMPs determine how the solute is distributed in the water close to the membrane. OMPs with charge opposite to the membrane charge will be attracted by the membrane, while OMPs with the same charge will be repelled [29]. The membrane surface charge is decided by its functional group deprotonation, which is influenced by the membrane material, solution pH, and solution composition [30]. While the charges of OMPs is determined by the dissociation constants of the molecules (pKa or pKb values) and the pH of the solution [31].

Specific solute-membrane interactions can also have a significant impact on the removal of OMPs. Surface adsorption would occur when the solute exhibits an affinity for the membrane. Studies have shown that this mainly occurs on the surface of polymeric membranes, which are more hydrophobic. In the case of ceramic membranes, their stronger hydrophilicity leads to a less important effect of surface adsorption [32]. Some OMPs are adsorbed to plastic surfaces because of their affinity for membrane, thus increasing the rejection efficiency [29]. The degree of hydrophobicity can be measured by the octanol/water partition coefficient ( $K_{ow}$ ) of the OMPs. A higher log  $K_{ow}$  value resulting in higher hydrophobicity [33].

### **2.2.2 Ultrafiltration membrane**

Although UF membranes cannot reject OMPs by the size exclusion mechanism due to their relatively large pore sizes (10 – 100 nm) and MWCO (>10000 Da) [4], they can still remove 30% - 50% of some OMPs such as testosterone, oxybenzone, and androstenedione [34]. Overall, the ability of UF to separate OMPs is very limited, it is impossible to effectively remove OMPs by UF alone in water treatment.

UF membranes can be classified according to their material into polymeric and ceramic membranes. Polymeric materials such as cellulose acetate (CA) or polypropylene (PP) are common materials due to their cost-effectiveness, strong mechanical properties, and the flexibility in designing porosity[35]. Nevertheless, polymeric membranes are not capable of operating in extreme conditions, such as high temperatures and aggressive chemical environments [7]. Additionally, membrane fouling caused by the accumulation of insoluble impurities is a major problem of polymer membranes, resulting in reduced treatment efficiency [36].

Ceramic membranes are synthesized from inorganic substances including TiO<sub>2</sub>, Al<sub>2</sub>O<sub>3</sub> or ZrO<sub>2</sub>. These materials possess exceptional chemical, mechanical, and thermal stability, which allows the membranes to maintain excellent treatment efficiencies under harsh conditions [37]. To be specific, most ceramic membranes can withstand temperatures of up to 280°C. They also exhibit excellent corrosion resistance against organic solvents and high acid or alkaline solution. Higher mechanical strength gives them a longer lifespan than polymeric membranes [7]. However, ceramic membranes have drawbacks mainly related to their fabrication cost and fragility [38].

### **2.2.3 Membrane fouling**

Membrane fouling is a significant challenge that limiting the performance of membrane filtration. The substances in the feed solution may create fouling either on the membrane surface or within its pores [39]. These substances including particulates, organic compounds, and microorganisms. Membrane fouling can reduce membrane flux and raise transmembrane pressure (TMP), and hence leading to higher separation resistance, decreased productivity, and changes in membrane selectivity. This problem impacts the rejection efficiency of the targeted contaminants in the feed water, thus lower the permeate quality and flux recovery.

Fouling usually forms through four ways: 1). Lipophilic macromolecules like proteins and humic acids adsorbed onto the membranes driven by surface energy and thermodynamic equilibrium; 2). Pores blockage caused by colloids and particles; 3). Inert or active colloids

build up layer by layer on the outer surface of the membrane to form cake layers; 4). A layer of highly concentrated macromolecular adjacent to the membrane surface solidifies under concentration polarization to form gel [39].

In order to mitigate the effect of fouling on membrane performance, various physical and chemical membrane cleaning methods are available. The most common physical cleaning method is backwashing, where water is pumped back from the permeate side and the forcing solution to pass through the membrane in the opposite direction [40]. This method can efficiently remove fouling from the membrane surface and can its efficiency be enhanced by increasing the backwash pressure [41]. However, it may not be very effective for fouling that accumulates deep in the membrane pores. In comparison, chemical cleaning methods involve the use of different chemicals to dissolve the fouling directly or weaken the cohesive forces between the membrane surface and fouling [40]. Different types of fouling require specific cleaning agents, for instance, acid cleaners are effective in eliminating inorganic fouling such as  $\text{CaCO}_3$ , while alkaline cleaners are used to reduce organic and biological fouling, also, surfactants can be used to remove colloids [42].

### **2.3 Advanced oxidation processes**

AOPs are effective methods for the degradation of OMPs in water treatment. AOPs can be achieved via activating oxidants to generate reactive species including hydroxyl radical ( $\cdot\text{OH}$ ), superoxide radicals ( $\text{O}_2^{\cdot-}$ ), singlet oxygen ( $^1\text{O}_2$ ), sulfate radicals ( $\text{SO}_4^{\cdot-}$ ), and so on. The high oxidizing ability of the radicals allows them to degrade OMPs more efficiently into  $\text{CO}_2$ ,  $\text{H}_2\text{O}$ , and other less harmful substances [9]. AOPs can be classified depending on how the oxidant is activated. These include catalytic AOPs represented by the Fenton and Fenton-like AOPs, ultraviolet-based photocatalytic AOPs, Ozone-based AOPs, and electrochemical AOPs, etc. Some of the AOPs are already well developed and operating at full-scale in water treatment plants, such as the AOPs based on Fenton reaction, UV and  $\text{O}_3$  [43]. [Table 1](#) lists the advantages and disadvantages of 6 kinds of common AOPs.

**Table 1: Comparison of the advantages and disadvantages of various AOPs**

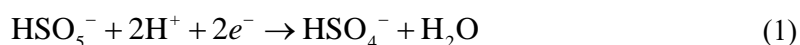
<b>AOP</b>	<b>Advantages</b>	<b>Disadvantages</b>
Fenton reaction	<ul style="list-style-type: none"> <li>No potential formation of bromated by product,</li> <li>Easy to operate,</li> <li>Nonselective oxidation of organics.</li> </ul>	<ul style="list-style-type: none"> <li>Iron sludge generation,</li> <li>Low pH (&lt;2.5) is required to keep iron in solution,</li> <li>pH adjustment will increase operating cost.</li> </ul>
Photo-Fenton reaction	<ul style="list-style-type: none"> <li>More efficient in generating hydroxyl radicals compared to Fenton reaction,</li> <li>Operates under mild conditions.</li> </ul>	<ul style="list-style-type: none"> <li>Iron sludge generation,</li> <li>sensitivity to pH variations.</li> </ul>
O <sub>3</sub> /UV	<ul style="list-style-type: none"> <li>Highly effective in inactivating bacteria and viruses,</li> <li>Shorter retention time.</li> </ul>	<ul style="list-style-type: none"> <li>Potential bromated by product</li> <li>UV light penetration can be obstructed by turbidity</li> <li>Energy and cost intensive processes</li> <li>Compounds such as nitrate can interfere with the absorbance of UV light</li> </ul>
H <sub>2</sub> O <sub>2</sub> /UV	<ul style="list-style-type: none"> <li>No potential formation of bromated by product,</li> <li>Can be applied in situ.</li> </ul>	<ul style="list-style-type: none"> <li>Potential bromated by product</li> <li>UV light penetration can be obstructed by turbidity</li> <li>Compounds such as nitrate can interfere with the absorbance of UV light</li> </ul>
Sonolysis	<ul style="list-style-type: none"> <li>Very effective for degrading persistent organic pollutants.</li> </ul>	<ul style="list-style-type: none"> <li>High energy requirements,</li> <li>Low mineralization,</li> <li>Limited to laboratory scale.</li> </ul>
Electrochemical oxidation	<ul style="list-style-type: none"> <li>Versatile and selective,</li> <li>Minimal chemical consumption,</li> <li>Can be operated continuously.</li> </ul>	<ul style="list-style-type: none"> <li>Requires intensive electricity input,</li> <li>Potential for electrode fouling,</li> <li>Limited to certain types of pollutants</li> </ul>

The Fenton reaction is a typical AOP system that generates hydroxyl radicals through the coupling of a transition metal with an oxidizing agent. The basic Fenton reaction uses Fe<sup>2+</sup> to catalyze the formation of <sup>•</sup>OH from H<sub>2</sub>O<sub>2</sub> under an acidic environment. H<sub>2</sub>O<sub>2</sub> is a strong oxidize agent with approximately 1.8V reduction potential [44]. However, its oxidizing ability is enhanced with the Fenton reaction, since <sup>•</sup>OH has a higher redox potential up to 2.5V [11]. <sup>•</sup>OH can also be generated from other method such as photo-Fenton (H<sub>2</sub>O<sub>2</sub>/UV) or electro-Fenton process [45]. Hydroxyl radical is a highly reactive and strong oxidizing agent, which is widely used in the HR-AOPs and plays an important role in degrading OMPs in water treatment. Although <sup>•</sup>OH is effective in degrading OMPs, its main disadvantage is that the reaction works

best at low pH levels ( $\text{pH} < 4$ ), which is due to the maximum catalytic capacity of  $\text{Fe}^{2+}$  is around  $\text{pH} = 3$  and precipitation of iron at high pH [46].

In the last decade, peroxydisulfate (PDS,  $\text{S}_2\text{O}_8^{2-}$ ) and peroxymonosulfate (PMS,  $\text{HSO}_5^-$ ) were introduced as new chemical oxidizers for the degradation of OMPs. They can be activated in various ways to produce  $\text{SO}_4^{\bullet-}$ ,  $\bullet\text{OH}$ , and other reactive species.  $\text{SO}_4^{\bullet-}$  is a stronger one-electron oxidant with an oxidation potential of 2.5 - 3.1V [13], which indicates it can degrade organic matter more effectively than  $\bullet\text{OH}$ , thus some researchers consider AOPs using PDS or PMS as a potential alternative to  $\text{H}_2\text{O}_2$ -based AOPs. PDS has a symmetrical structure, the distance of its O-O bond is 1.497 Å and contains 140 kJ/mol of bond energy [47]. In comparison, PMS, with an O-O bond distance of 1.453 Å, contains higher bond energy between 140-213.3 KJ/mol [47]. In addition, the asymmetric structure of PMS allows it to be activated more easily than PDS, which results in more electron transport [13]. For these reasons, it is more effective to use PMS as a reactant for sulfate-AOPs.

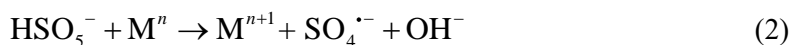
The  $\text{HSO}_5^-$  ion is a derivate of  $\text{H}_2\text{O}_2$  in which one H-atom is replaced by a  $\text{SO}_3^-$  group. It has an oxidation potential of 1.82 V, similar to that of  $\text{H}_2\text{O}_2$  (1.8V). PMS has been commonly used as a pool disinfectant along with chlorine because of its strong oxidizing properties. It can also partially degrade some organic compounds based on Eq.(1) [12].



However, although PMS exhibits strong oxidizing properties, its direct reaction rate with most OMPs is too slow, so it needs to be activated to generate reactive species.

### 2.3.1 Activation of PMS

PMS can be activated by various methods, including thermal, UV, metal or metal oxide. The fission of the O-O bond in the structure of PMS is the crucial mechanism for activating PMS [16]. In the case of metal and metal oxide activation, the mechanism they are used as electron acceptors to reduce PMS [13]. The reduction mechanism is shown in Equation (2).



Previous experiments have shown that  $\text{Co}^{2+}$  has the best ability to activate PMS among all the transition metals [17]. However,  $\text{Co}^{2+}$  is a potential carcinogen that can threaten consumers' health if its salts and oxides enter the water supply [18].

Noble metals have received more attention because of their outstanding capability to induce catalytic reduction [13]. Ahn et al., compared the activation of PMS by fixing four noble metals, Pd, Pt, Au, and Ag on  $\text{Al}_2\text{O}_3$  support and concluded that Pd had the highest OMPs removal

efficiency [13]. Later on, Feng et al., compared the efficiency of Pd/Al<sub>2</sub>O<sub>3</sub> - PMS with other common oxidants, including H<sub>2</sub>O<sub>2</sub>, PDS and copper-iron bimetallic activator for the degradation of 1,4-dioxane, and the results demonstrated that the highest degradation efficiency of organic matter was achieved using Pd-activated PMS [14]. They proposed that Pd<sup>0</sup> served as a real catalyst instead of an electron donor since the increase of Pd<sup>2+</sup> was not significant. The mechanism is described as the equation (3).

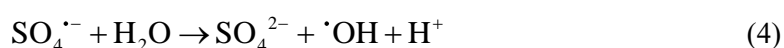


### 2.3.2 Functional reactive species in the PMS-Pd/UF system

The presence of SO<sub>4</sub><sup>•-</sup> and reactive oxygen species (ROS) including hydroxyl radical (•OH), superoxide radicals (O<sub>2</sub><sup>•-</sup>), singlet oxygen (<sup>1</sup>O<sub>2</sub>) were reported to be found in the activated PMS system.

#### 2.3.2.1 Hydroxyl radical

•OH is the common reactive species has been found within the activated-PMS system. •OH was found to be present in many experiments using metal/metal oxide, UV, alkaline, ozone, etc. to activate PMS and was verified to dominate in the degradation of OMPs such as sulfamethoxazole, haloacetonitriles, and atrazine [48, 49, 50]. It can be formed either by the fission of PMS (Eq.(3)), or the transformation of SO<sub>4</sub><sup>•-</sup> as the Equation (4) [15]. The later reaction is also strongly affected by pH. At pH greater than 12, the reaction is promoted in the forward direction and •OH becomes the dominant radical in the system. Whereas at pH less than 7, the reaction is inhibited and SO<sub>4</sub><sup>•-</sup> is mainly present in the system [51].



#### 2.3.2.2 Sulfate radical

Sulfate radicals can be generated from PMS through Eq.(3). Sulfate radical-based advanced oxidation processes (SR-AOPs) have been widely studied in recent years. Several studies have shown that SR-AOPs have the potential to be an alternative to HR-AOPs in water treatment. Advantages of SO<sub>4</sub><sup>•-</sup> over •OH include: i) it has a higher reduction potential of 2.6 - 3.1 V [13]; ii) it can function in a wider pH range (3-9), while •OH only works at acidic conditions [13]; iii) it has a longer half-life span of 30 - 40 μs than •OH of only 1 μs, which results in the increase of interaction and mass transfer between OMPs and SO<sub>4</sub><sup>•-</sup> [52]. As a result, it is expected that SO<sub>4</sub><sup>•-</sup> will show a similar or better ability to degrade OMPs from water compared to •OH.

#### 2.3.2.3 Superoxide radical

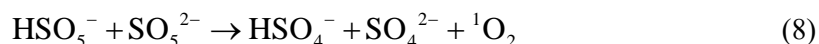
The excess of •OH produces H<sub>2</sub>O<sub>2</sub> and then triggers the generation of O<sub>2</sub><sup>•-</sup> (Eq.(5)-(7)) [16, 53].

The presence of  $O_2^{\cdot-}$  was detected, which plays a role in the degradation of various types of OMPs such as bisphenol A and Trichloroethylene in the PMS catalytic system. [54, 55].



#### 2.3.2.4 Singlet oxygen

Another notable reactive species in the PMS catalytic system is  $^1O_2$ , which is a nonradical process and follows a distinct oxidation mechanism in comparison to the radicals mentioned earlier. Despite its lower reduction potential (2.2V) and a short half-life of 2  $\mu s$  compared to  $\cdot OH$  and  $SO_4^{\cdot-}$ ,  $^1O_2$  demonstrates increased reactivity with electron-rich compounds like olefins, phenols, polycyclic aromatic, and heterocycles [53,56]. This is because the  $\pi$ -antibonding orbital of  $^1O_2$  makes it more prone to acquiring an electron pair, thereby making it more likely to undergo electrophilic addition reactions with electron-rich organics, rather than single-electron transfer reactions [57].  $^1O_2$  can be formed through two methods, one involves the decomposition of PMS (Eq.(8)), while the other way is  $O_2^{\cdot-}$  acts as an intermediate species in the evolution process of  $^1O_2$  (Eq.(9)).



All of the above reactive species have the ability to degrade various OMPs, but their importance in the PMS-Pd/UF system is required for further investigation.

#### 2.3.3 Effect of water constituents on the degradation of organic matter by PMS

Natural water bodies such as surface water, groundwater, brackish water and seawater all have complex compositions in which a large number of ions and natural organic matter (NOM) react with the PMS and with the above mentioned reactive species, thus affecting the performance of the PMS in oxidizing the target OMPs [12,15].

Among numerous kinds of ions,  $Cl^-$  is present in large quantities in different water bodies and has been reported to inhibit the degradation of OMPs by activated PMS in several studies [14,58,59,60]. The reason is that  $Cl^-$  reacts with  $SO_4^{\cdot-}$  as shown in the Equation (10)-(11), resulting in the formation of less reactive  $Cl\cdot$  and  $Cl_2\cdot^-$  [12,59]. However, it was also found that

although chloride concentrations around 5 mM reduced the removal efficiency, high concentrations (500 mM) increased the rate constant by a factor of 4-15. Br<sup>-</sup> and I<sup>-</sup> were also found to have similar effects [61].



HCO<sub>3</sub><sup>-</sup>, CO<sub>3</sub><sup>2-</sup>, PO<sub>4</sub><sup>3-</sup>, NO<sub>3</sub><sup>-</sup>, and SO<sub>4</sub><sup>2-</sup> also quench sulfate and hydroxyl radicals. For instance, HCO<sub>3</sub><sup>-</sup> and CO<sub>3</sub><sup>2-</sup> can be oxidized into HCO<sub>3</sub><sup>•</sup> and CO<sub>3</sub><sup>•-</sup> and hence reduce the overall degradation capacity [62]. Yao et al. investigated the effect of various anions on the degradation of Orange II by PMS catalyzed by Fe@C-BN and found that they suppressed the removal efficiency in the order of S<sub>2</sub>O<sub>3</sub><sup>2-</sup> > HCO<sub>3</sub><sup>-</sup> > CO<sub>3</sub><sup>2-</sup> > Cl<sup>-</sup> > HPO<sub>4</sub><sup>2-</sup> > NO<sub>3</sub><sup>-</sup> > SO<sub>4</sub><sup>2-</sup> [63]. They also mentioned that in addition to anions reacting directly with the reactive species, anions also compete with the target OMPs for adsorption on the catalyst surface, leading to catalyst site clogging [62,63].

NOM is a complex mixture of naturally occurring organic matter in water and soil environments, usually including humic and fulvic acids recovered from vegetation and soils [64]. The concentration of NOM varies depending on the source of the water and its surroundings, with concentrations ranging from 2 to 10 mg/L in surface water and groundwater [65]. Studies have indicated that NOM has a negative impact on the removal of OMPs by active PMS. Similar to anions, NOM also competes with the target OMPs for various reactive species and reduces the available oxidant [14]. In addition, some NOMs rich in phenolic hydroxyl and carboxyl groups, e.g., hyaluronic acid, tend to be adsorbed on the surface of the catalyst, hindering the contact between oxidants, pollutants, and active sites [60].

## 2.4 Integration of AOP and UF membranes

The mechanisms and limitations of using both membrane filtration and AOP for the removal of OMPs are described in the previous section. To summarize, AOP chemically breaks down OMPs, however, the metal catalysts used in this process can remain in the treated water and cause contamination. Membrane filtration physically separates the OMPs from water, but other contaminants like NOM often results in membrane fouling and reduces efficiency. In addition, the concentrate stream produced from membrane filtration containing a high level of OMPs requires further chemical treatment. To overcome their limitations and improve treatment efficiency, integrating them by means of catalytic membranes is a promising approach.

### 2.4.1 Catalytic membrane

Catalytic membrane is a type of membrane that combines a catalytic reaction with a separation process in a single unit. The preparation process involves immobilizing the catalyst on the membrane surface and/or in the pores, thus omitting the need for catalyst recovery in conventional AOPs. Although both polymer and ceramic membranes can be used to prepare catalytic membranes, the metal oxide-based separated top layer of the ceramic membrane is more convenient for deposition of the metal/metal oxide-based catalytic layer [66]. This is because ceramic membranes are also made of metal oxides, the affinity between the metal-based membranes surface and the metal-based catalysts make immobilization of the catalysts easier [66]. Moreover, ceramic membranes exhibit greater chemical stability than their polymeric counterparts, allowing them to resist the oxidation of res during the catalytic separation process [67]. As a result, the metal catalysts are not prone to leakage into water when supported by ceramic membranes. For example, Álvarez et al. immobilized Co onto  $\gamma$ -Al<sub>2</sub>O<sub>3</sub>, and after two hours of catalytic ozonation experiments, about 0.10% of Co leaked [68]. Thus, they concluded that the catalyst is stable on ceramic membrane surface.

Membrane fouling caused by organics is also significantly mitigated with the addition of AOPs. Park et al. compared the degradation of NOM with and without AOP in an experiment using  $\gamma$ -Al<sub>2</sub>O<sub>3</sub> based membrane coated with Fe<sub>2</sub>O<sub>3</sub> nanoparticles [69]. The findings revealed a 15% reduction in flux due to fouling when utilizing the catalytic membrane, as opposed to a more substantial 30% decrease in flux observed in the test employing the pristine membrane. In addition, OMPs could be degraded in catalytic membrane filtration, thus reducing the requirement for subsequent treatment of concentrate water.

Another advantage provided by the UF membrane is its dense and fine membrane structure, facilitating optimal contact between OMPs, oxidants, and catalysts. This enhances mass transfer, subsequently boosting the efficiency of AOP in the degradation of OMPs [5]. Due to the extremely short half-life of the free radicals, the free radicals can only persist in the space near the surface of the solid catalyst rather than dispersing throughout the entire solution. This significantly reduces the probability of reactions between the free radicals and the targeted pollutant. In catalytic membranes, however, the nanoscale space provided by the UF pores would increase the probability of the reaction due to the enhanced mass transfers of radicals and OMPs [70].

### 2.4.2 Atomic layer deposition

In order to uniformly immobilize an ultrathin catalyst layer onto the membrane surface and in the pores, one of the most promising techniques is ALD, a specialized form of chemical vapor

deposition (CVD). CVD involves the reaction of vapor-phase precursors that are introduced into a reaction chamber, where they undergo chemical reactions to form a solid film on the substrate surface. Although CVD creates finely controlled films and deposit microstructures, ALD has additional advantages for producing catalytic membranes. ALD can deposit highly uniform and conformal films on surfaces characterized by nanoscale aspect ratios [71]. It also operates at a lower temperature than CVD to prevent damage to the membrane [72].

In previous studies, ALD has successfully grown a wide range of materials, including transitions and noble metal elements, as well as their oxides, nitrides, and sulfides 错误!未找到引用源。 . Lu et al. were the first to use ALD technique to load Pd nanoparticles on Al<sub>2</sub>O<sub>3</sub>-based ceramic membranes, and the synthesized catalytic membrane exhibited improved oxidation ability for p-nitrophenol [20].

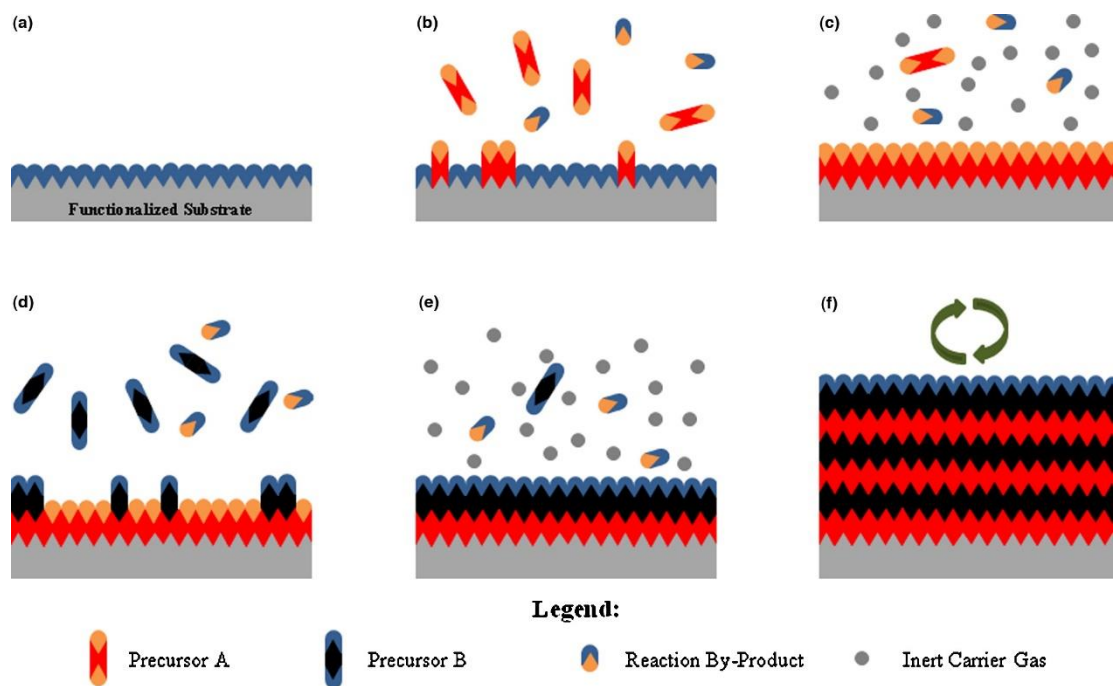


**Figure 2:** Schematic of ALD process. (a) Substrate surface has natural functionalization or is treated to functionalize the surface. (b) Precursor A is pulsed and reacts with surface. (c) Excess precursor and reaction by-products are purged with inert carrier gas. (d) Precursor B is pulsed and reacts with surface. (e) Excess precursor and reaction by-products are purged with inert carrier gas. (f) Steps 2–5 are repeated until the desired material thickness is achieved 错误!未找到引用源。 .

## 3 Methodology

### 3.1 Chemicals and reagents

All chemicals and reagents were used as received. Potassium peroxymonosulfate ( $\text{KHSO}_5 \cdot 0.5\text{KHSO}_4 \cdot 0.5\text{K}_2\text{SO}_4$ ,  $\geq 99.0\%$ ) and sodium thiosulfate ( $\text{Na}_2\text{S}_2\text{O}_3$ ,  $\geq 99.0\%$ ) were purchased from Sigma-Aldrich (Germany). Acids and bases for pH adjustment and membrane cleaning, including: HCl (37 - 38%, Honeywell's Fluka), NaOH ( $\geq 97\%$ , Merck, Germany), and NaClO (60-285g/L active chlorine, Merck, Germany). Salts used in the tests including: NaCl ( $\geq 99\%$ , Sigma-Aldrich, Germany),  $\text{NaHCO}_3$  ( $\geq 99\%$ , Merck, Germany),  $\text{NaH}_2\text{PO}_4$  ( $\geq 99\%$ , Merck, Germany),  $\text{Na}_2\text{SO}_4$  ( $\geq 99\%$ , Sigma-Aldrich, Germany),  $\text{NH}_4\text{Cl}$  ( $\geq 99.5\%$ , Sigma-Aldrich, Germany), NaBr ( $\geq 99\%$ , Sigma-Aldrich, Germany). Organic reagents used for the quenching experiments including: methanol ( $\text{CH}_3\text{OH}$ ,  $\geq 99.97\%$  hypergrade for LC-MS LiChrosolv®, Merck, Germany), ethanol absolute ( $\text{C}_2\text{H}_5\text{OH}$ ,  $\geq 99.8\%$  AnalaR NORMAPUR®, VWR Chemicals, Netherlands), furfuryl alcohol ( $\text{C}_5\text{H}_6\text{O}_2$   $\geq 98\%$ , Sigma-Aldrich, Germany), L(+)-ascorbic acid ( $\text{C}_6\text{H}_8\text{O}_6$ ,  $\geq 99.0\%$ , Merck, Germany), and tert-butanol ( $(\text{CH}_3)_3\text{COH}$ ,  $\geq 99.5\%$ , Sigma-Aldrich, Germany). Potassium iodide (KI,  $\geq 99.5\%$ , Honeywell's Fluka) was used for the iodometric method for the determination of PMS.

The Dutch Ministry of Infrastructure and Water Management lists 11 compounds as target substances to monitor the effectiveness of novel treatment technologies for removal of OMPs from wastewater [21]. Seven common pharmaceuticals out of these OMPs were selected for this study. The information of 7 types of soluble OMPs were purchased from Sigma-Aldrich (Germany) is listed in Table 2.

### 3.2 Ultrafiltration membrane information

The tubular ceramic ultrafiltration membrane was made of  $\alpha$ -alumina with a pore size of 20 nm as indicated by the specification of the manufacturer, CoorsTek. It had an inner diameter of 7 mm, an outer diameter of 10 mm, and a length of 8 cm. The interior surface area and exterior surface area were 0.0017 and 0.0025m<sup>2</sup>, respectively.

The porosity of the membrane ( $\varepsilon$ ) is 23.6%, was estimated using the following equation (12):

$$\varepsilon = \frac{\omega_1 - \omega_2}{A \times \ell \times d_w} \quad (12)$$

Where  $\omega_1$  (kg) is the membrane weight after immersed in the ultrapure water for 12 hours, whereas  $\omega_2$  (kg) is the dry membrane weight, A (m<sup>2</sup>) is the membrane surface area,  $\ell$  (m) is the membrane thickness, and  $d_w$  (998 kg/m<sup>3</sup>) is the density of water.

The retention time ( $t$ , (s)) was calculated by using the equation (13):

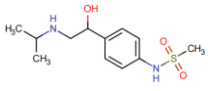
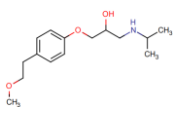
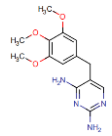
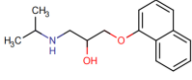
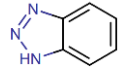
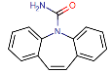
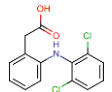
$$t = \frac{n}{\frac{Q \times 10^{-3}}{3600}} \times \varepsilon \quad (13)$$

Where  $n = 1.3 \times 10^{-6}$  m is the thickness of the filtration layer, which was measured from cross-sectional image of the membrane (Figure S 1) obtained from Scanning electron microscopy (SEM),  $Q$  (LMH) is the flux, and  $\varepsilon$  (%) is the porosity.

### 3.3 ALD-Pd method

Palladium ALD was performed using alternating exposures to  $\text{Pd}(\text{hfac})_2$  as the precursor and formalin as the co-reactant. Ultrahigh purity nitrogen (99.999%) was used as purging gas. The ALD timing sequences can be expressed as  $t_1$ – $t_2$ – $t_3$ – $t_4$  second (s). Where  $t_1$  is the exposure time for the precursor,  $t_2$  is the purge time following the precursor exposure,  $t_3$  is the exposure time for the co-reactant,  $t_4$  is the purge time following the exposure to the co-reactant. The

**Table 2:** Properties of the selected OMPs

Name	Molecular structure	Molecular weight (g/mol)	Log $K_{ow}$	Charge (at pH 7)	Application
Sotalol (SOT)		272	-0.39	+	beta blocker
Metoprolol (MP)		267	1.88	+	beta blocker
Trimethoprim (TMP)		290	0.59	+	antibiotic
Propranolol (PPL)		259	3.45	+	beta blocker
Benzothiazole (BT)		119	2.01	0	corrosion inhibitor
Carbamazepine (CBZ)		236	2.45	0	anticonvulsant
Diclofenac (DIC)		296	4.55	-	anti-inflammatory

timing sequence for coating Pd was typically 1:1:1:1 s [73]. Based on the previous experiments, the time sequence in this study was set to 30-30-40-30 s. The Pd(hfac)<sub>2</sub> was held in a stainless-steel bubbler maintained at 70 °C. The ALD reactor was kept at 200 °C to prevent the reabsorption of the Pd(hfac)<sub>2</sub>. First, Pd(hfac)<sub>2</sub> with a 0.5 L/min flow rate was sent through the bubbler with 0.5 L/min N<sub>2</sub> for 30 s. Then the purging step required 30 s for 1 L/min N<sub>2</sub> flow. Next, formalin with a 0.7 L/min flow rate passed through the bubbler with 0.3 L/min N<sub>2</sub> for 40 s. Finally, repeat the purging step once, and one cycle of ALD was done. In our experiments, the selected ALD cycles were 60 times.

### 3.4 OMPs removal experiments

For each experiment, 2.5 mL of a 1 mg/L stock solution of OMPs was added to 500 mL of ultrapure water, resulting in a concentration of 5 µg/L of each OMPs. After mixing, a 5 mL sample was taken to determine the actual concentration of OMPs. Then 2 mL of 10 mM PMS solution was added and the pH was adjusted to 7 (or 2.5 and 11) by 0.5 mM NaOH and HCl solution. The experiments started with feeding the mixed solution to the membrane for 3 minutes to achieve a stable fixed flux under a certain pressure. The 5 mL of samples used for determine OMPs were taken at t = 5, 15, 25, 35, 45 minutes from the permeate stream, after that 50 µL 40 mM Na<sub>2</sub>S<sub>2</sub>O<sub>3</sub> were added into the samples to stop the reaction. The concentration of OMPs were tested by Liquid chromatography–mass spectrometry (LC-MS, ACQUITY UPLC I-Class, Xevo TQ-S micro fitted with the ESI). 1.5 mL of samples used for determine PMS were collected from the permeate stream at t = 10, 20, 30, 40, 50 minutes, and from the feed solution at t = 0, 50 minutes. The PMS concentrations were quantified by adding 1.5 mL of 1g/L KI to the samples, and tested by the UV-Vis under 352nm [74]. The calibrated curve of PMS concentration with UV absorption spectra is shown in [Figure S 8](#).

### 3.4.1 Experiments set-up

All the OMPs removal tests were completed by using the dead-end constant pressure set-up as shown in Figure 3. The rotation speed of the pump was fixed at 150 RPM, and the value of flux could be calculated from the change in electronic balance readings over a certain period of time. With the rotational speed fixed, the flux can be adjusted to the desired value for the experiment by adjusting the pressure valve at the feed end. Due to no fouling formed during the filtration, flux can maintain constant at a fixed pressure.

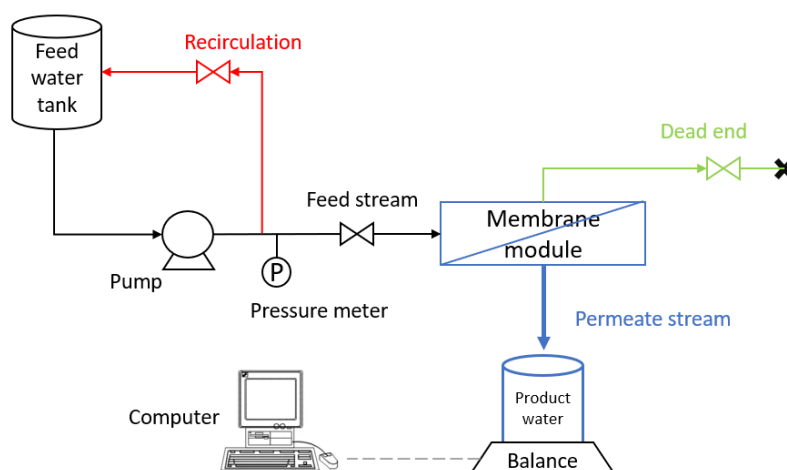


**Figure 3:** Reactor set-up for OMPs removal tests and quenching experiments. The concentrate stream was closed and forced all the water to be filtered by the membrane.

### 3.4.2 Effect of different factors on OMPs removal efficacy

The OMPs removal efficiency can be affected by flux, pH, PMS concentration, and presence of ions. Tests at different flux conditions were performed in order to calculate and adjust the kinetic constants for residence time calculations, and also to evaluate whether the membrane can remove contaminants quickly at high flux. The initial selection of PMS was 40  $\mu\text{M}$  (mass concentration was 35.7  $\mu\text{g/L}$ ), which was equal to the total concentration of OMPs (35  $\mu\text{g/L}$ ). To further understand the relationship between PMS dosage and Pd loading, other PMS dosages were tested. The pH was chosen to examine the performance of PMS-Pd/UF in removing OMPs under acidic, neutral and alkaline conditions. Therefore, experiments in a variety of conditions will be performed. The different operational parameters are shown in Table 3.

Regarding the ions tests, natural water contains complex anions such as  $\text{Cl}^-$ ,  $\text{Br}^-$ ,  $\text{CO}_3^{2-}$ ,  $\text{NH}_4^+$ ,  $\text{SO}_4^{2-}$ ,  $\text{NO}_3^-$ ,  $\text{PO}_4^{3-}$  which can obstruct the degradation of OMPs by competing with radical species produced in AOP. In this study, the most common anions ( $\text{Cl}^-$ ,  $\text{HCO}_3^-$ ,  $\text{SO}_4^{2-}$ , and  $\text{ClO}^-$ ) found in natural water were chosen and added at 1 mM concentration to the OMPs solution

[75].

**Table 3: Operational parameters for OMPs tests**

Factors	Flux (LMH)	pH (-)	PMS concentration ( $\mu\text{M}$ )	Ions
Flux tests	30/100/200/500/900	7	40	-
pH tests	30	2.5/7/10	40	-
PMS tests	30	7	20/40/80	-
Ions tests	30	7	40	1 mM $\text{Cl}^-$ / $\text{HCO}_3^-$ / $\text{SO}_4^{2-}$ / $\text{ClO}^-$

### 3.4.3 Other water matrices

In this part of the experiment, water matrices were replaced from ultrapure water to surface water, simulated brine water, and simulated brackish water. Their properties can be found in Table 3.

**Table 4: Properties of simulated brackish water, simulated brine water and river water**

Water matrices	$\text{Cl}^-$ (ppm)	$\text{Br}^-$ (ppm)	$\text{NH}_4^+$ (ppm)	$\text{NO}_3^-$ (ppm)	$\text{PO}_4^{3-}$ (ppm)	$\text{SO}_4^{2-}$ (ppm)	TDS (ppm)
Brackish water	1160	2.2	8.6	8.9	11.3	1766	4573
Brine water	5800	11	43	44.5	56.5	8830	22867
Surface water	COD: 155 ppm		TOC: 23.73 ppm		Turbidity: 0.354 NTU		568

### 3.4.4 12 hours experiment

To examine the long-term stability, 12 hours test was applied with 40  $\mu\text{M}$  PMS and 5  $\mu\text{g/L}$  OMPs at pH 7 and 30 LMH of flux. The reason that the experiment was only 12 hours long was due to the limitation of the opening hours of the laboratory and the fact that the reactor could not be run unsupervised. 6 samples were taken at  $t = 2, 4, 6, 8, 10, 12$  hours.

## 3.5 Reactive species determination experiments

Quenching experiments were conducted to find out which kind of reactive specie that determines the oxidation of OMPs by Pd-catalyzed PMS. The scavengers including methanol, ethanol, tert-butanol (TBA), furfuryl alcohol (FFA), and L-ascorbic acid (AA) were used to eliminate the specific reactive specie, as shown in Table 4 [76,77,78,79]. Based on the kinetic constants of scavengers with different ROS, the main ROS can be attributed to the one which has less inhibited effect on OMPs degradation when scavenger was added to feed OMPs

solution. The operational parameters were set at the default condition, which was 30 LMH flux, 40  $\mu\text{M}$  PMS and pH 7. The dosing concentration of scavengers were 0.4 and 40 mM, which were 10 and 1000 times of the PMS level, respectively [76]. Table 4 summarizes the second-order rate constants between scavengers and reactive species. All tests were completed by using the constant pressure set-up as shown in Figure 3.

**Table 5: Second-order rate coefficients between various scavengers and reactive species**

Scavenger	Reactive species scavenged	$\kappa^{\bullet\text{OH}}$ ( $\text{M}^{-1}\text{S}^{-1}$ )	$\kappa_{\text{SO}_4^{\bullet-}}$ ( $\text{M}^{-1}\text{S}^{-1}$ )	$\kappa_{\text{O}_2^{\bullet-}}$ ( $\text{M}^{-1}\text{S}^{-1}$ )	$\kappa^{\text{O}_2}$ ( $\text{M}^{-1}\text{S}^{-1}$ )
Methanol	$\bullet\text{OH}$ , $\text{SO}_4^{\bullet-}$	$9.7 \times 10^8$	$1.1 \times 10^7$	-	$3.89 \times 10^3$
Ethanol	$\bullet\text{OH}$ , $\text{SO}_4^{\bullet-}$	$2.0 \times 10^9$	$4.1 \times 10^7$	-	-
TBA	$\bullet\text{OH}$	$4.8 \times 10^9$	$8.3 \times 10^5$	-	$1.8 - 3.0 \times 10^3$
FFA	$^1\text{O}_2$	$1.5 \times 10^{10}$	$1.3 \times 10^{10}$	$3.5 \times 10^3$	$1.2 \times 10^8$
AA	$\text{O}_2^{\bullet-}$	$4.5 \times 10^9$	-	$5.4 \times 10^6$	-

### 3.6 Surface Pd and pores Pd determination experiments

As reported, ALD is conformal coating technology that allows to grow Pd on the membrane surface and in the pores [19]. It is assumed that the grown catalysts in the 20 nm pores can enhance the degradation of OMPs due to the nanoconfined effect and prolonging the contact time [6]. To study the effect of Pd in the pores, the kinetic constants of the OMPs degradation by surface and pore Pd was compared. When using the set-up of Figure 3, water could contact the Pd inside the membrane pores and on the membrane surface, so the OMPs removal efficiency could be obtained when the catalytic reaction occurs both on the surface and inside the pores. To determine the contribution of Pd on the surface to the system's performance, the

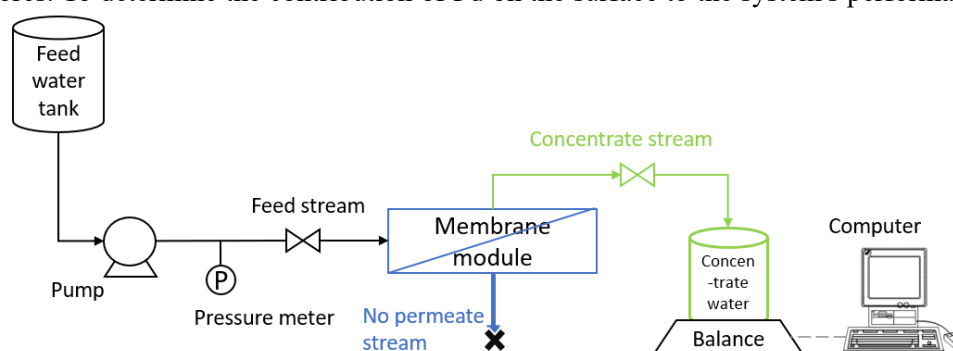


**Figure 4:** Reactor set-up for surface catalysts tests. The permeate stream was closed and all of the water could not enter the pores of the membrane, so PMS would not be activated by the Pd in the pores.

set-up shown in Figure III can be used. The permeate stream was closed and concentrate stream was opened as shown in Figure 4, then the degradation of OMPs was assumed to be only achieved by the catalysts on the surface. The operational parameters were at the default conditions. The retention time of feed water in the membrane module were set at 15, 30, 50, 70, 90 seconds. 2 samples were collected at  $t = 30$  and 50 minutes.

## 4 Results and discussions

### 4.1 OMPs degradation by Pd/UF activated PMS

To examine the effectiveness of PMS activated by Pd-coated ultrafiltration membranes (PMS-Pd/UF) in the removal of OMPs, the pristine membrane without immobilized Pd (C0) and the catalytic membrane coated with 60 ALD cycles (C60) were tested. Figure 5 shows the efficiency of OMPs removal by C0 and C60 under conditions with and without the presence of PMS. Under the conditions of using the pristine membrane without PMS, it can be observed that only 42.4% of BT and 17.8% of DIC were removed. This may be attributed to their adsorption by the polyvinyl chloride (PVC) pipeline used in the experiments. Yu et al.'s experiments revealed that PVC microplastics adsorb BT through the mechanism of hydrophobic interaction, electrostatic force and non-covalent bonds [80]. Tseng et al. also found that DIC can be consistently adsorbed on a variety of plastics including PVC due to its very high log  $K_{ow}$  value (4.55), which means that it is highly hydrophobic [81]. In addition, some studies have indicated that microorganisms can degrade BT and DIC. Therefore, the microorganisms present in pipelines may also contribute to the removal of these substances to some extent [82].

In the case when pristine membrane and 40  $\mu\text{M}$  PMS were coupled, the PMS was unactive due to no presence of catalysis like Pd. As observed in Figure 4, the degraded DIC and BT increased to 74.5% and 70.4%, respectively, with simultaneous removal of 15%-20% of CBZ, SOT, and TMP. This may be due to the fact that PMS can directly decompose OMPs through a non-radical pathway. In addition, it has been reported that PMS can also self-decompose to

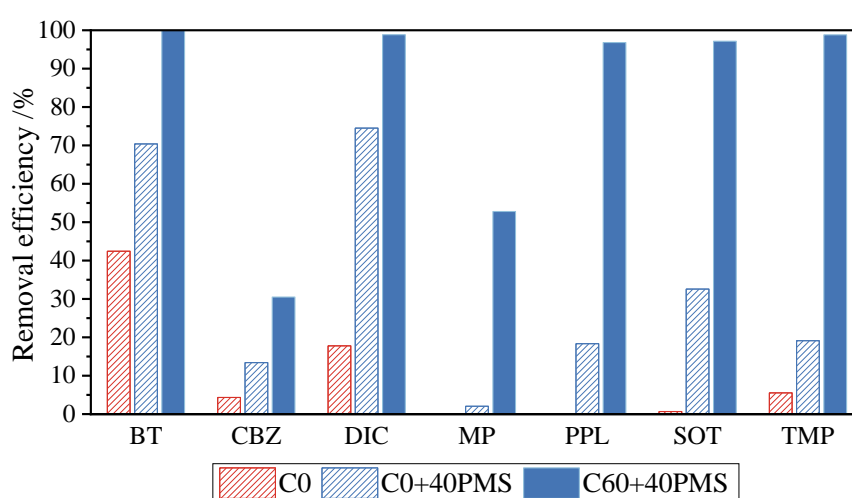


**Figure 5:** Comparison of the average removal efficiency of OMPs within 50 minutes for pristine membrane (C0) with and without the addition of 40 $\mu\text{M}$  PMS, and 60-cycle membrane (C60) with the addition of 40 $\mu\text{M}$  PMS. Default condition: pH = 7, flux = 30 LMH.

generate reactive species in a slow rate to oxidize OMPs [83,84]. When C60 was used and PMS was added, PMS was activated to produce reactive species. The oxidizing ability of the system was enhanced for all OMPs, with removal efficiencies exceeding 97% for five of them.

Moreover, the degradation of OMPs by H<sub>2</sub>O<sub>2</sub>-Pd/UF was also investigated. Figure S 2 shows that, except for more than 95% of BT and TMP were removed, the degradation efficiency of the other types of OMPs by the addition of H<sub>2</sub>O<sub>2</sub> was lower than that when the same dosage of PMS was used. Thus, PMS is more effective than H<sub>2</sub>O<sub>2</sub> when using Pd as the catalyst.

The 12 hours long-term stability test is shown in Figure S 3. The removal efficiency of PMS-Pd/UF for five OMPs, BT, DIC, PPL, SOT and TMP, remained above 80% during the first four hours. It reached more than 90% in the 6 to 12 hours, and did not present a decline in performance.

#### 4.1.1 Effect of flux

Figure 6a demonstrates the removal of seven OMPs by PMS-Pd/UF at 30, 100, 200, 500 and 900 LMH, while Figure 6b shows the PMS consumption and the retention time of PMS molecule passing the membrane at various fluxes. From Figure 6b, it can be observed that at a flux of 30 LMH, the retention time of the feed water in the filtration layer was 0.37 seconds (Computed using Eq.(13), Table 6). In this case, 98.5% of the PMS was decomposed to produce reactive species catalyzed by Pd, which in turn resulted in 97-100% of the five types of OMPs were decomposed as shown in Figure 6a. However, an increase in flux hindered sufficient contact between PMS and the catalyst, particularly noticeable when the flux rose from 200 LMH to 500 LMH corresponding to the retention time of 0.056s and 0.022s (Eq.(13), Table 6), respectively. As a result, PMS consumption decreased from 74.4% to 41.0%. And can be seen from Figure 6a, the overall removal efficiency of OMPs declined with an increase in flux.

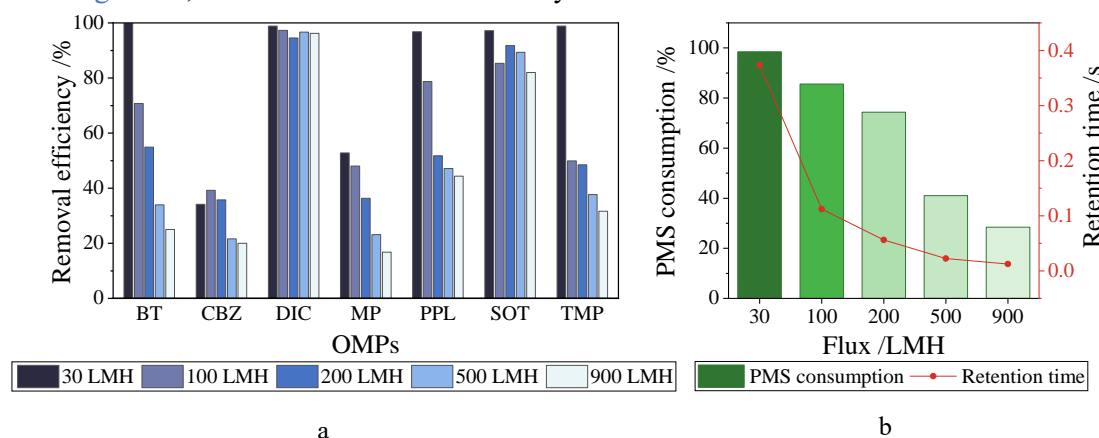


**Figure 6:** (a) The average removal efficiency of OMPs within 50 minutes at flux = 30, 100, 200, 500, and 1000 LMH; (b) PMS consumption and retention time at five fluxes. Experiments conditions: 40  $\mu$ M PMS and pH = 7.

Therefore, it can be concluded that PMS-Pd/UF was more effective at low flux.

#### 4.1.2 Effect of PMS dosage

The dosage of PMS affected both the degradation efficiencies of the PMS-Pd/UF system in degrading OMPs. Figure 7a compares the results of OMPs removal using 20, 40, and 80  $\mu\text{M}$  PMS. When the dosage of PMS was reduced from the 40 to 20  $\mu\text{M}$ , the removal efficiency of all OMPs decreased. The PPL was affected with degradation efficiency reducing from 96.8% to 21.2%, while CBZ and MP were only decomposed by about 10%. However, as can be seen in the Figure 7b, PMS was fully reacted in 50 minutes, indicating that 20  $\mu\text{M}$  PMS could not provide enough reactive species to oxidize the OMPs such as PPL, CBZ and MP in this PMS-Pd/UF system.

When the PMS dosage was increased from 40 to 80  $\mu\text{M}$ , more reactive species were produced. Hence, the degradation efficiencies of CBZ and MP, which were originally difficult to remove, were elevated to 69.0% and 78.7%. However, it is noteworthy that the removal efficiency of TMP decreased from 98.8% to 87.2%. This could be attributed to the insufficient catalyst loading, preventing the full activation of PMS in the case with 80  $\mu\text{M}$  PMS [85]. The excess of PMS reacted with the strongly oxidizing  $\text{SO}_4^{\bullet-}$  and  $\cdot\text{OH}$  to produce the less oxidizing  $\text{SO}_5^{\bullet-}$  with a reduction potential of 0.82V (Eq.(14)(15)), which in turn inhibited the degradation of OMPs [60,86].

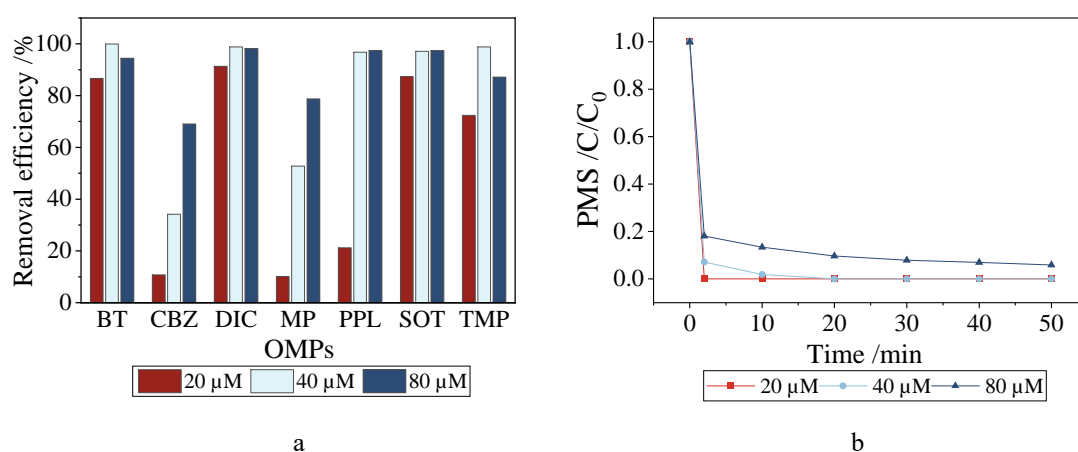


**Figure 7:** (a) The average removal efficiency of OMPs with the addition of 20, 40, and 80  $\mu\text{M}$  PMS; (b) Changes in the PMS residual concentration ratio ( $C/C_0$ ) with time at 20, 40, and 80  $\mu\text{M}$  PMS dosages; Experiments conditions: Flux = 30 LMH and pH = 7

From Figure 7b, when 80  $\mu\text{M}$  PMS was added, it was never completely consumed during the 50-minute experiment. Thus, it can be concluded that 80  $\mu\text{M}$  PMS was slightly excessive in this system. Although more PMS dosage enhanced the removal efficiency for CBZ and MP, the lack of catalysts allowed excess PMS to consume a fraction of the reactive species, resulting in suppressed degradation of the OMPs. This result was also found in other studies that used metals or UV to activate PMS to oxidize organic contaminants [87,88].

#### 4.1.3 Effect of pH

pH is an important factor affecting the performance of PMS-Pd/UF. This is attributed to the fact that the pH level induces changes in the structures of the OMPs, leading to distinct charges. Consequently, the reaction rate with oxidants is modified [60]. Additionally, pH variations impact the distribution and proportion of reactive species in the solution, thereby affecting the removal of OMPs [89]. Figure 8a compares the efficiency of PMS-Pd/UF in eliminating OMPs at pH=2.5, 7 and 11. The degradation ratio of OMPs was inhibited at pH 2.5 and 11. Also, according to the variation of the remaining concentration of PMS under different pH conditions shown in Figure 8b, only about half of the PMS was consumed at pH 2.5 and 11. At pH=11, 69.8% of the SOT was degraded and the other 6 OMPs were removed between 10% and 35%. The reason for this could be that the pKa of PMS is 9.4 [90]. When the pH exceeded 9.4,  $\text{SO}_5^{2-}$  replaced  $\text{HSO}_5^-$  as the dominant form in the solution, thereby affecting the reaction in Eq. (3) and reducing the generation of  $\text{SO}_4^{\cdot-}$  and other reactive species. Additionally, the reduction potential of  $\text{SO}_5^{2-}$  is only 1.22 V, which is lower than the 1.75 V of  $\text{HSO}_5^-$ , indicating that its oxidizing capacity is weaker [14,91]. When the pH was decreased from 7 to 2.5, PMS still existed in the form of  $\text{HSO}_5^-$ , so the ability of PMS to directly oxidize BT and DIC was not inhibited. Thus at pH 2.5, 95% of BT and DIC were still degraded. In conclusion, it can be

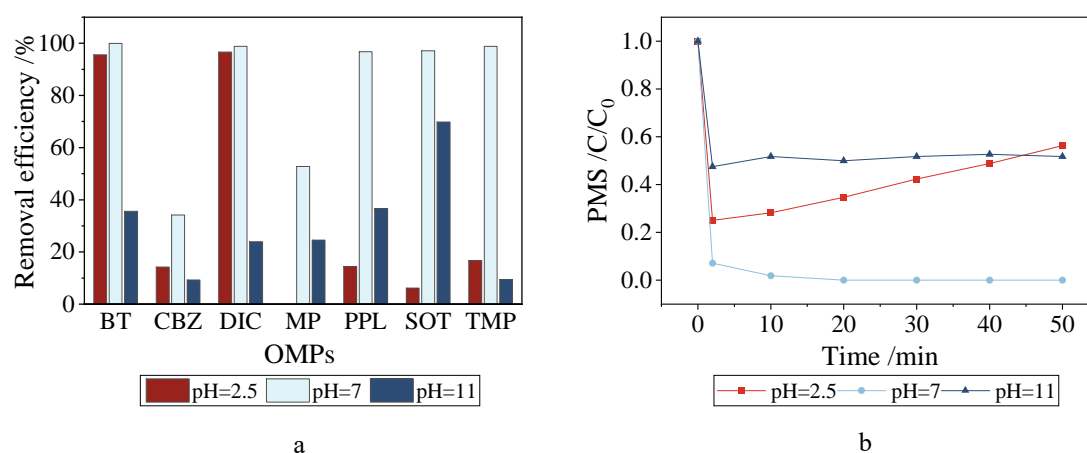


**Figure 8:** (a) The average removal efficiency of OMPs at pH = 2.5,7, and 11; (b) Changes in the PMS residual concentration ratio ( $C/C_0$ ) with time at pH = 2.5, 7 and 11; Experiments conditions: 40  $\mu\text{M}$  PMS and 30 LMH flux.

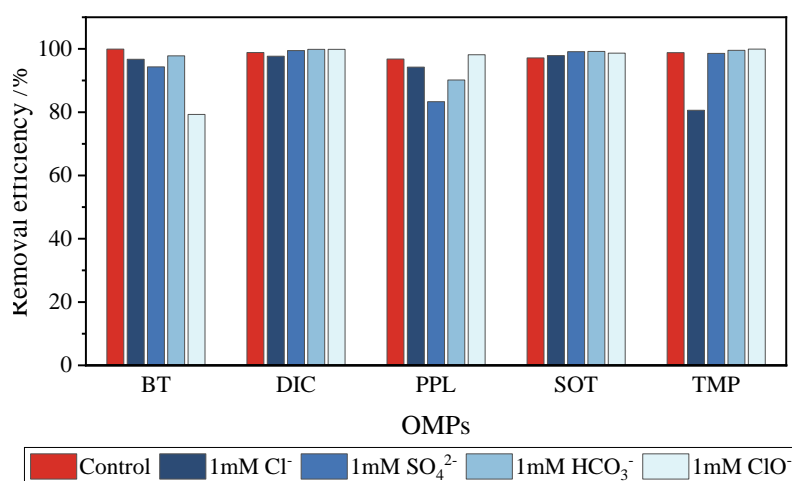
suggested that the PMS-Pd/UF system is more suitable for treating water with a pH of 7.

#### 4.1.4 Effect of natural water constituents

Figure S 5a demonstrates the impact of 1 mM  $\text{Cl}^-$ ,  $\text{SO}_4^{2-}$ ,  $\text{HCO}_3^-$ ,  $\text{ClO}^-$  separately on the OMPs removal efficiency in the PMS-Pd/UF system. As shown in Figure 9, the presence of these anions had limited impact on degradation of the 5 OMPs. The addition of 1 mM  $\text{Cl}^-$  decreased the removal efficiency of TMP from 98.8% to 80.6%, while it had no significant influence on the other four OMPs. This phenomenon may be due to the fact that the addition of  $\text{Cl}^-$  quenched some of the original reactive species present in the system and generated the less oxidizing  $\text{Cl}^\cdot$  and  $\text{Cl}_2^\cdot$  (Eq.(10)-(11)) [12]. The other three anions also had a similar inhibitory effect.  $\text{SO}_4^{2-}$  and  $\text{HCO}_3^-$  restrained the breakdown of PPL, while  $\text{ClO}^-$  suppressed the decomposition of BT, although their removal efficiencies remained higher than 80%. In general, 1 mM ions had little impact on the performance of PMS-Pd/UF system.

After replacing the ultrapure water with the simulated brackish and brine water having 50 mM and 250 mM of total anions, the increase in ions concentration resulted in a greater inhibitory effect on the degradation of OMPs as shown in Figure 10a. In brackish water, PMS-Pd/UF still exhibited promising oxidation on DIC, PPL and SOT, reaching more than 96.8%, whereas the removal efficiency of TMP dropped to 65%.

In brine with much higher ionic levels, the removal efficiencies of all OMPs decreased largely compared to those in brackish water, except for DIC, which still maintained at 97%. Figure 10b



shows the variation of PMS concentration with time in different water matrices. It can be seen

**Figure 9:** The average removal efficiency of OMPs in the presence of 1 mM  $\text{Cl}^-$ , 1 mM  $\text{SO}_4^{2-}$ , 1 mM  $\text{HCO}_3^-$ , 1 mM  $\text{ClO}^-$  and without any ions (control group). Experiments conditions: 30 LMH flux, 40  $\mu\text{M}$  PMS and pH = 7.

that the consumption of PMS decreases as the ion content increases, from 95% in brackish water to 70% in brine water. This may be due to the competition of reaction between ions and OMPs and thus weakened the oxidation degradation, as mentioned in section 2.3.3 [63].

When river water containing NOM (TOC = 23.73 ppm) was used, the decomposition of MP, PPL and TMP was more strongly suppressed, and other types of OMPs were not notably affected. Studies have suggested that NOM competes with OMPs for reactive species and thus inhibits OMPs removal efficiency [14].

Overall, PMS-Pd/UF was less affected when treating the water containing 50 mM total anions, while its performance deteriorated with increasing ion concentration. In addition, higher concentrations of NOM also reduced the OMPs removal efficiency.

## 4.2 Determination of the functional reactive species

Figure 11a shows the effect of adding 0.4 mM of MeOH and EtOH separately (10 times the PMS concentration) to PMS-Pd/UF on the removal efficiency of OMPs. Although MeOH has a fast reaction rate with  $\cdot\text{OH}$  ( $9.7 \times 10^8 \text{ M}^{-1}\text{S}^{-1}$ ) and  $\text{SO}_4^{\cdot-}$  ( $1.1 \times 10^7 \text{ M}^{-1}\text{S}^{-1}$ ) (Table 5), the results showed in that only the degradation of TMP, CBZ, and MP was more noticeably inhibited, in which TMZ decreased from 98% to 80%. Compared with MeOH, the reaction rate between EtOH and both  $\cdot\text{OH}$  ( $2.0 \times 10^9 \text{ M}^{-1}\text{S}^{-1}$ ) and  $\text{SO}_4^{\cdot-}$  ( $4.1 \times 10^7 \text{ M}^{-1}\text{S}^{-1}$ ) were faster, while its inhibitory effect on the degradation of OMPs was more obvious. It can be seen that the degradation efficiency of PPL was reduced from 95% to 43%, while TMP dropped from 80% to 11%, and also CBZ and MP reached a low removal level less than 10%. Another reason for the more apparent inhibitory effect of EtOH is its dielectric constant of 24, which is lower than

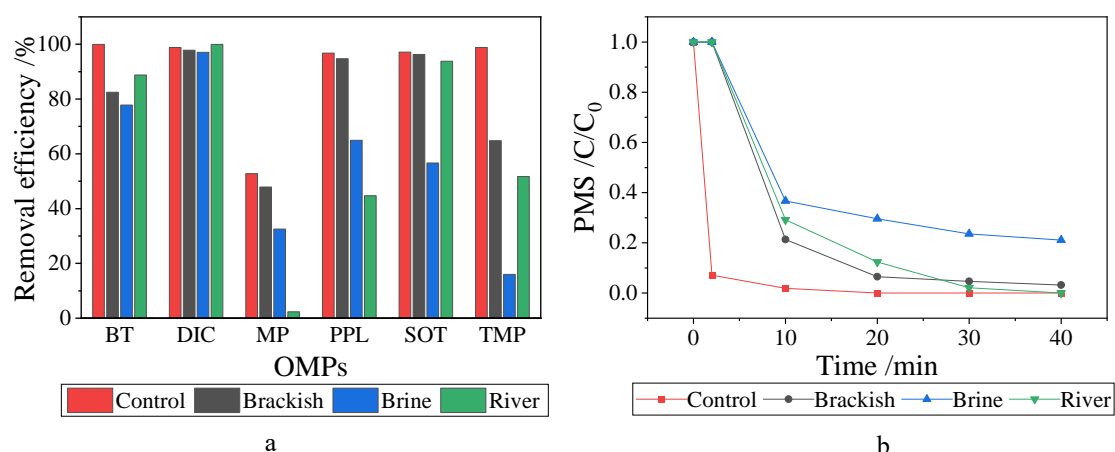


**Figure 10:** (a) Final removal efficiency of OMPs by PMS-Pd/UF in ultrapure water (control), brackish water, brine water, and river water after 50 min of reaction.

(b) PMS residual concentration ratio ( $C/C_0$ ) in ultrapure water (control), brackish water, brine water, and river water over time. Experiments conditions: 30 LMH flux, 40  $\mu\text{M}$  PMS, and  $\text{pH} = 7$ .

that of MeOH (33). This results in a higher affinity between EtOH and the Pd/Al<sub>2</sub>O<sub>3</sub> surface, making EtOH prone to hinder the contact between PMS and the catalytic sites, thereby inhibiting the degradation of OMPs [14].

From Figure 11b, when using TBA, which mainly quenches  $\cdot\text{OH}$  ( $4.8 \times 10^9 \text{ M}^{-1}\text{S}^{-1}$ ) while reacting more slowly with  $\text{SO}_4^{\cdot-}$  ( $8.3 \times 10^5 \text{ M}^{-1}\text{S}^{-1}$ ), the results of OMPs elimination was similar to that with the addition of EtOH. Therefore, based on the above results, it can be concluded that both  $\cdot\text{OH}$  and  $\text{SO}_4^{\cdot-}$  contributed to the degradation of TMP, CBZ, and MP, in which  $\cdot\text{OH}$  played a more important role.

In the presence of FFA as a quencher for  $^1\text{O}_2$ , it can be observed from Figure 11c that its inhibitory effect was not distinctly different from adding an equal amount of TBA. Therefore,

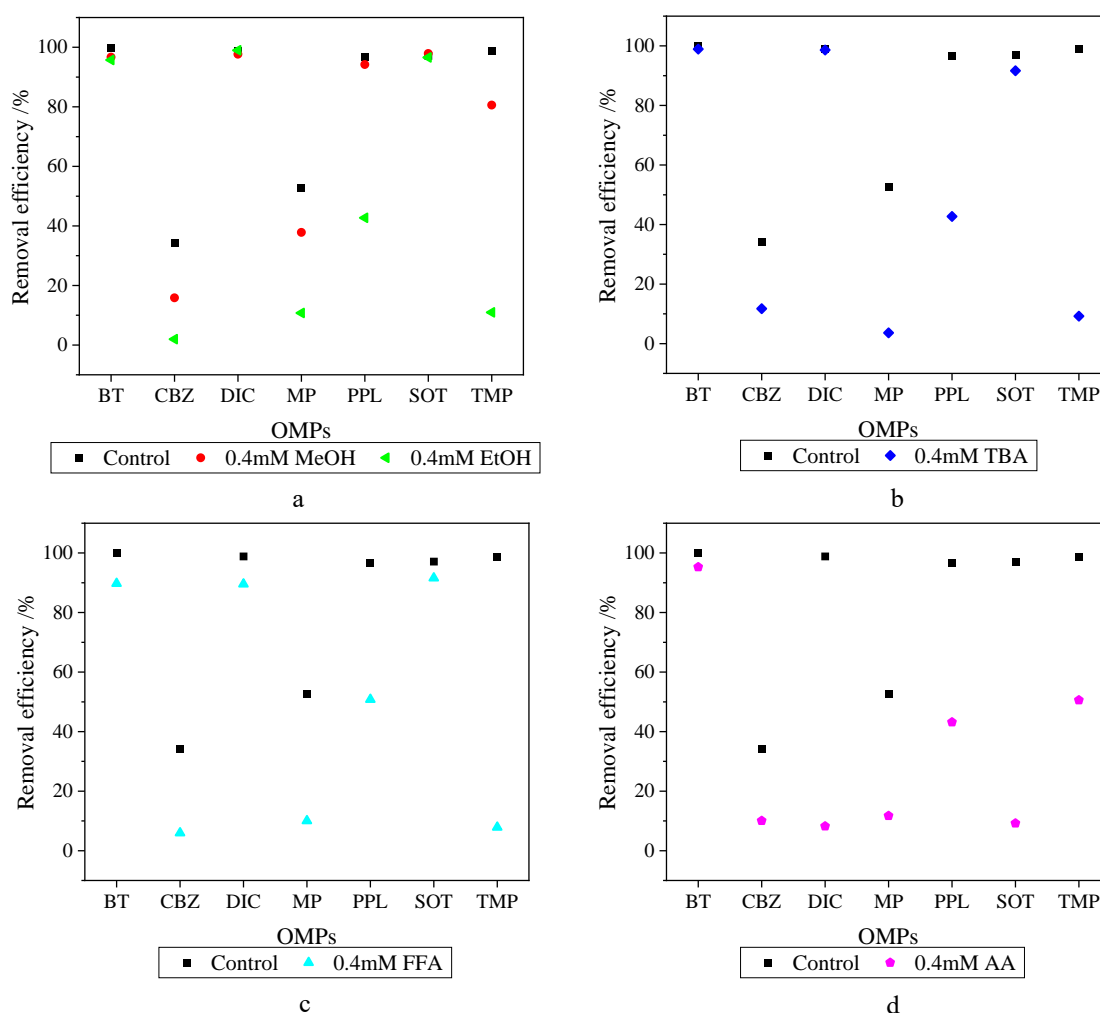


**Figure 11:** (a) Removal efficiency of OMPs in the absence of scavenger (control) and with 0.4 mM of methanol (quench  $\cdot\text{OH}$ ,  $\text{SO}_4^{\cdot-}$ ), ethanol ( $\cdot\text{OH}$ ,  $\text{SO}_4^{\cdot-}$ ); (b) OMPs removal efficiency in the control group and with 0.4 mM of tert-butanol ( $\cdot\text{OH}$ ); (c) OMPs removal efficiency in the control group and with 0.4 mM of furfuryl alcohol ( $^1\text{O}_2$ ); (d) OMPs removal efficiency in the control group and with 0.4 mM of and L-ascorbic acid ( $\text{O}_2^{\cdot-}$ ); Experiments condition: 30 LMH of flux, 40  $\mu\text{m}$  PMS, pH 7.

the role of  $^1\text{O}_2$  in the PMS-Pd/UF system was very limited. However, the removal of OMPs was inhibited when  $\text{O}_2^{\cdot-}$  was eliminated by AA. Figure 11d shows that the removal efficiency of DIC and SOT, which could not be reduced by the use of other scavengers, was inhibited, and their removal efficiencies decreased to about 10%. This suggested that the degradation of DIC and SOT is mainly dominated by  $\text{O}_2^{\cdot-}$ . As reported by Zhao et al., the removal of DIC was inhibited when scavenger for  $\text{O}_2^{\cdot-}$  was added in the PMS +  $\text{MnO}_2\text{-Bi}_2\text{O}_3$  system. The electron spin resonance (EPR) results in their study also indicated that the quantity of  $\text{O}_2^{\cdot-}$  was greater than that of  $\cdot\text{OH}$  and  $\text{SO}_4^{\cdot-}$  [92].

Moreover, AA reacted with both  $\cdot\text{OH}$  ( $4.5 \times 10^9 \text{ M}^{-1}\text{S}^{-1}$ ) and  $\text{O}_2^{\cdot-}$  ( $5.4 \times 10^6 \text{ M}^{-1}\text{S}^{-1}$ ) at a fast rate, but it could not react with  $\text{SO}_4^{\cdot-}$ . Figure 11d shows that 45% of TMP was removed in the addition of AA, which can be attributed to the presence of  $\text{SO}_4^{\cdot-}$ . Thus,  $\text{SO}_4^{\cdot-}$  and  $\cdot\text{OH}$  played equal roles in degrading TMP, which was also verified in the study using Co-activated PMS by Liu et al [93].

The addition of 0.4 mM (10 times of PMS level) of various scavengers still failed to inhibit the degradation of BT and 50% of PPL. This is because a lower ratio of scavenger to substrate can result in an inconspicuous quenching effect [14]. Therefore, scavengers were added at a concentration of 40 mM (1000 times PMS) to achieve a higher inhibitory effect, and the results are depicted in Figure 12. The degradation efficiency of PPL decreased from 96% to 14% when the MeOH concentration was increased by 100 times, while the degradation of PPL was completely stopped by the same dosage of EtOH. This indicates that both  $\cdot\text{OH}$  and  $\text{SO}_4^{\cdot-}$  promoted to the decomposition of PPL.

After the addition of various scavengers at a dosage of 40 mM, BT was still removed by over 80% (Figure 12). However, in some systems where PMS is activated using other methods like

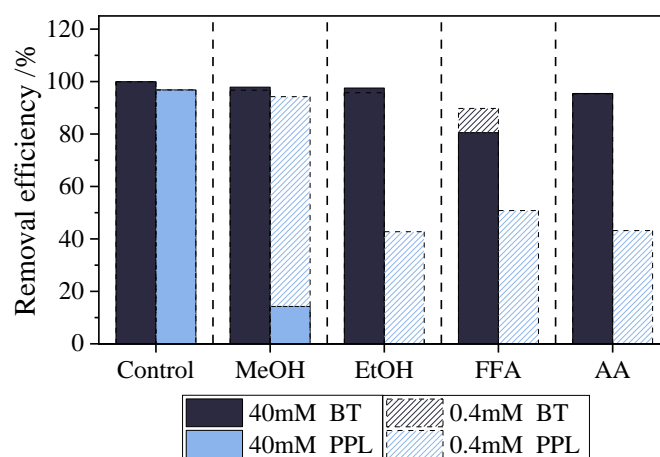


**Figure 12:** Removal efficiency of BT and PPL in the absence of scavenger (control) and with 40 mM of methanol (quench  $\cdot\text{OH}$ ,  $\text{SO}_4^{\cdot-}$ ), ethanol ( $\cdot\text{OH}$ ,  $\text{SO}_4^{\cdot-}$ ), furfuryl alcohol ( $^1\text{O}_2$ ), and L-ascorbic acid ( $\text{O}_2^{\cdot-}$ ); Experiments condition: 30 LMH of flux, 40  $\mu\text{m}$  PMS, pH 7.

Fe/TiO<sub>2</sub> and ozone/ultrasound, the degradation of BT can be significantly inhibited by scavengers such as EtOH and TBA [94,95]. This result further corroborated the discussion in Section 4.1, leading to the conclusion that in this PMS-Pd/UF system, approximately 80% of BT removal was not attributed to the effect of AOP, but rather resulted from direct oxidation by PMS, pipeline adsorption, and microbial activities.

### 4.3 Role of Pd coated on the surface and in the pores

Figure 13a shows the removal efficiency of OMPs solely by the Pd on the membrane surface at different retention times. When the contact time was the longest (90s), only about 45% of PPL was degraded, and for other OMPs were all below 25%. In contrast, as shown in Figure S 7, with a similar retention time (85 s), 95% of the five OMPs were removed under the combined effect of the catalysts inside the pores and on the surface. Figure 13b presents the pseudo-second-order kinetic models based on the average concentration changes of seven OMPs in both cases. The rate constants for surface Pd versus pores and surface Pd were 0.012 min<sup>-1</sup> and 4.3018 min<sup>-1</sup>, respectively. Thus, in the PMS-Pd/UF system, the catalytic effect within the membrane pores dominated the removal of OMPs, while the contribution of surface Pd was very limited. Thus, in the PMS-Pd/UF system, the catalytic effect within the membrane pores dominated the removal of OMPs, while the contribution of surface Pd was very limited. This is because the 20 nm pores can confine OMPs and reactive species at the nanoscale. Through the confinement of the membrane pores and channels, there is a greater chance of contact between reactive species and OMPs due to minimal diffusion distance and mass transfer enhancement, resulting in a more complete reaction [6]. This finding highlights the promotion of AOP performance by the 20nm UF.

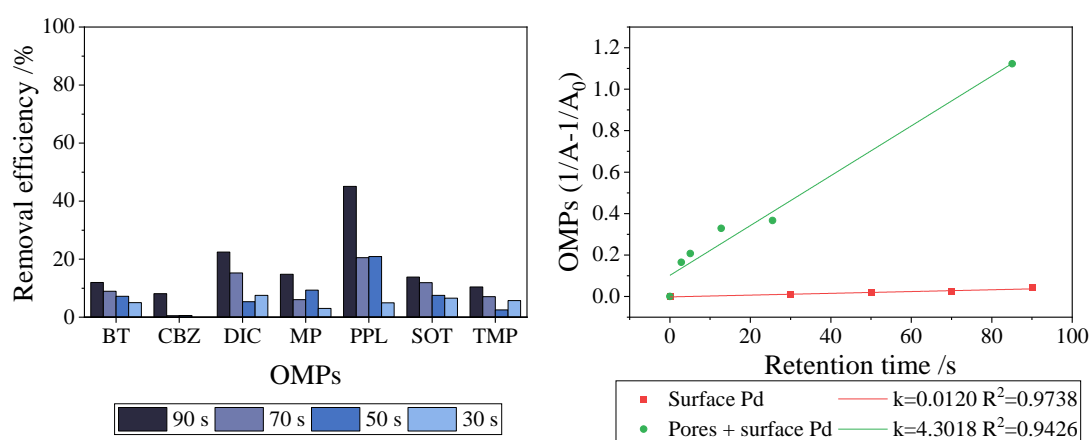


**Figure 13:** (a) OMPs removal efficiency by surface catalysis only under various retention times. (b) Pseudo-second-order kinetic models for the 7 OMPs average degradation by surface catalysis only (Experiments condition: pH=7, 40 $\mu$ m PMS, retention time= 30, 50, 70, 90s); And by both the pores and surface catalysis (Experiments condition: pH=7, 40 $\mu$ m PMS, retention time= 3, 5, 13, 26, 85s)

## 5 Limitations and recommendations

One of the uncertainties in this study was how much Pd actually was loaded to membrane after 60 ALD cycles. Although Elam et al. measured that each ALD cycle produces a catalytic layer of Pd with a thickness of 0.02 nm, its mass or density remains unknown [73]. The weight of Pd is very important in practice because it will affect the cost of the catalytic membrane. And for the research, it is mentioned in [section 4.1.2](#) that the C60 membrane could not fully activate 80 $\mu$ M of PMS, so if a proper ratio of Pd loading to the PMS dosage can be found, the operation performance of the PMS-Pd/UF system can be enhanced. It is reported that Pd can be dissolved from the support material by some hash solution, and then the loading of Pd can be measured by inductively coupled plasma optical emission spectrometry (ICP-OES) [96]. Another technique, High-angle annular dark-field scanning transmission electron microscopy (HAADF-STEM), provides a resolution better than 0.05 nm, might be possible to test the depth of Pd growth inside the membrane pores. Hence perhaps the loading of Pd on UF membrane can be determined by these ways.

As mentioned above, the loading of Pd is important for the membrane performance. Therefore, UF membranes coated with various ALD cycles are also suggested to have a further study. In addition, in this study, it shown that the catalysis coated in the pores have a prominent impact on the degradation of OMPs, compared to the catalysis grown on the top membrane surface. But how the pore size would affect the degradation of OMPs in PMS-Pd/UF is unknown.

The reactive species determination by various scavengers were also suggested to be repeated at a low concentration. Because the concentration of scavengers in this study was at 10 and 1000 times higher than 40  $\mu$ m of PMS concentration, this perhaps led to the results that all induced reactive species were consumed in a very short time. But if the concentration of scavengers was reduced to a low level, perhaps a much significant difference in the inhibition of OMPs removal can be found with different quenchers.

Moreover, more research is needed for the application of PMS-Pd/UF in practical water treatment. Although the performance of this system was studied in simulated brackish and brine water, the composition of actual water bodies is more complex, which may introduce more uncertainties in the removal efficiency of OMPs. Furthermore, one river water sample was used in this experiment to assess the impact of NOM, but in real applications, the system would need to handle source water with varying concentrations and types of NOM and OMPs. Therefore, future studies may require testing with a broader range of actual water matrices.

Considering that PMS-Pd/UF was not effective in removing CBZ and MP in this study, thus it

may not be able to treat all kinds of OMPs in practical applications, resulting in a small amount of OMPs still remaining in the product water. Therefore, it is preferable to establish double barrier system in the practical to ensure the quality of the effluent. An ideal way is to set up activated carbon adsorption after PMS-Pd/UF, which is a common tertiary treatment for drinking water. It can further remove OMPs from the water, as well as tastes, odors, chlorine and fluorine which cannot be removed by PMS-Pd/UF to achieve better water quality.

## 6 Conclusion

This study investigated the efficiency of using Pd/UF to activate PMS for the removal of seven OMPs. Based on the results, the following conclusions were derived:

(1) The PMS-Pd/UF system demonstrated the capability to simultaneously remove over 95% of BT, DIC, PPL, SOT, and TMP at a flux of 30 LMH and with 40  $\mu\text{M}$  PMS. This efficiency was maintained consistently throughout the continuous 12-hour experiment. However, this system was not effective in degrading CBZ and MP.

(2) Increasing the PMS dosage from 40  $\mu\text{M}$  to 80  $\mu\text{M}$  did not promote the overall degradation of OMPs.

(3) The generation of reactive species from Pd-catalyzed PMS was inhibited at pH 2.5 and 11 due to the dissociation of PMS, indicating that PMS-Pd/UF was more suitable for treating water under neutral pH conditions.

(4) The presence of 1 mM  $\text{Cl}^-$ ,  $\text{HCO}_3^-$ ,  $\text{SO}_4^{2-}$ , and  $\text{ClO}^-$  did not have much effect on the system's performance. When the number of anions increased to more than 50 mM, it hindered the contact of PMS with the catalytic sites and thus reduced the removal efficiency of OMPs. NOM in river water can react directly with the reactive species, thus reducing the degradation of OMPs.

(5)  $\cdot\text{OH}$  and  $\text{SO}_4^{\cdot-}$  together promoted the degradation of PPL, TMP, CBZ and MP, while  $\text{O}_2^{\cdot-}$  dominated the degradation of SOT and DIC in this system. However, the removal of BT was mainly due to direct oxidation of PMS, pipeline adsorption and biological effect, rather than the effect of reactive species.

(6) The pores of UF provided more surface area available for Pd immobilization, while increasing the contact opportunities of Pd, PMS and OMPs through nano confinement, which in turn enhanced the efficiency of the oxidation reaction.

## 7 Reference

- [1] Borrull, J., Colom, A., Fabregas, J., Borrull, F., & Pocurull, E. (2021). Presence, behaviour and removal of selected organic micropollutants through drinking water treatment. *Chemosphere*, 276, 130023. <https://doi.org/10.1016/j.chemosphere.2021.130023>
- [2] Rozas, O., Vidal, C., Baeza, C., Jardim, W. F., Rossner, A., & Mansilla, H. D. (2016). Organic micropollutants (OMPs) in natural waters: Oxidation by UV/H<sub>2</sub>O<sub>2</sub> treatment and toxicity assessment. *Water Research*, 98, 109–118. <https://doi.org/10.1016/j.watres.2016.03.069>
- [3] Khanzada, N. K., Farid, M. U., Kharraz, J. A., Choi, J., Tang, C. Y., Nghiem, L. D., Jang, A., & An, A. K. (2020). Removal of organic micropollutants using advanced membrane-based water and wastewater treatment: A review. *Journal of Membrane Science*, 598, 117672. <https://doi.org/10.1016/j.memsci.2019.117672>
- [4] Chen, Z., Yang, B., Wen, Q., & Tang, Y. (2021). Application of potassium ferrate combined with poly-aluminum chloride for mitigating ultrafiltration (UF) membrane fouling in secondary effluent: Comparison of oxidant dosing strategies. *Chemosphere*, 274, 129862. <https://doi.org/10.1016/j.chemosphere.2021.129862>
- [5] Westermann, T., & Melin, T. (2009). Flow-through catalytic membrane reactors—Principles and applications. *Chemical Engineering and Processing: Process Intensification*, 48(1), 17-28. <https://doi.org/10.1016/j.cep.2008.07.001>
- [6] Zhang, B.T., Yan, Z., Liu, Y., Chen, Z., Zhang, Y., & Fan, M. (2023). Nanoconfinement in advanced oxidation processes. *Critical Reviews in Environmental Science and Technology*, 53(12), 1197–1228. <https://doi.org/10.1080/10643389.2022.21469815>
- [7] Hubadillah, S. K., Othman, M. H. D., Matsuura, T., Ismail, A. F., Rahman, M. A., Harun, Z., Jaafar, J., & Nomura, M. (2018). Fabrications and applications of low cost ceramic membrane from: A comprehensive review. *Ceramics International*, 44(5), 4538–4560. <https://doi.org/https://doi.org/10.1016/j.ceramint.2017.12.215>
- [8] Alresheedi, M. T., Barbeau, B., & Basu, O. D. (2019). Comparisons of NOM fouling and cleaning of ceramic and polymeric membranes during water treatment. *Separation and Purification Technology*, 209, 452–460. <https://doi.org/https://doi.org/10.1016/j.seppur.2018.07.070>
- [9] Żyła, R., Boruta, T., Gmurek, M., Milala, R., & Ledakowicz, S. (2019). Integration of advanced oxidation and membrane filtration for removal of micropollutants of emerging concern. *Process Safety and Environmental Protection*, 130, 67–76. <https://doi.org/https://doi.org/10.1016/j.psep.2019.07.021>
- [10] Titchou, F. E., Zazou, H., Afanga, H., el Gaayda, J., Ait Akbour, R., Nidheesh, P. V., & Hamdani, M. (2021). Removal of organic pollutants from wastewater by advanced oxidation processes and its combination with membrane processes. *Chemical Engineering and Processing - Process Intensification*, 169, 108631. <https://doi.org/https://doi.org/10.1016/j.cep.2021.108631>
- [11] Buxton, G. v, Greenstock, C. L., Helman, W. P., & Ross, A. B. (1988). Critical Review of rate constants for reactions of hydrated electrons, hydrogen atoms and hydroxyl radicals ( $\cdot\text{OH}/\cdot\text{O}^-$  in Aqueous Solution. *Journal of Physical and Chemical Reference Data*, 17(2), 513–886. <https://doi.org/10.1063/1.555805>

- [12] Ghanbari, F., & Moradi, M. (2017). Application of peroxymonosulfate and its activation methods for degradation of environmental organic pollutants: Review. *Chemical Engineering Journal*, 310, 41–62. <https://doi.org/10.1016/j.cej.2016.10.064>
- [13] Ahn, Y. Y., Yun, E. T., Seo, J. W., Lee, C., Kim, S. H., Kim, J. H., & Lee, J. (2016). Activation of Peroxymonosulfate by Surface-Loaded Noble Metal Nanoparticles for Oxidative Degradation of Organic Compounds. *Environmental Science and Technology*, 50(18), 10187–10197. <https://doi.org/10.1021/acs.est.6b02841>
- [14] Feng, Y., Lee, P.-H., Wu, D., & Shih, K. (2017). Surface-bound sulfate radical-dominated degradation of 1,4-dioxane by alumina-supported palladium (Pd/Al<sub>2</sub>O<sub>3</sub>) catalyzed peroxymonosulfate. *Water Research*, 120, 12–21. <https://doi.org/https://doi.org/10.1016/j.watres.2017.04.070>
- [15] Wang, J., & Wang, S. (2018). Activation of persulfate (PS) and peroxymonosulfate (PMS) and application for the degradation of emerging contaminants. In *Chemical Engineering Journal* (Vol. 334, pp. 1502–1517). <https://doi.org/10.1016/j.cej.2017.11.059>
- [16] Devi, P., Das, U., & Dalai, A. K. (2016). In-situ chemical oxidation: Principle and applications of peroxide and persulfate treatments in wastewater systems. *Science of The Total Environment*, 571, 643–657. <https://doi.org/https://doi.org/10.1016/j.scitotenv.2016.07.032>
- [17] Hu, P., & Long, M. (2016). Cobalt-catalyzed sulfate radical-based advanced oxidation: A review on heterogeneous catalysts and applications. *Applied Catalysis B: Environmental*, 181, 103–117. <https://doi.org/https://doi.org/10.1016/j.apcatb.2015.07.024>
- [18] Anipsitakis, G. P., Stathatos, E., & Dionysiou, D. D. (2005). Heterogeneous Activation of Oxone Using Co<sub>3</sub>O<sub>4</sub>. *The Journal of Physical Chemistry B*, 109(27), 13052–13055. <https://doi.org/10.1021/jp052166y>
- [19] Johnson, R. W., Hultqvist, A., & Bent, S. F. (2014). A brief review of atomic layer deposition: from fundamentals to applications. *Materials Today*, 17(5), 236–246. <https://doi.org/https://doi.org/10.1016/j.mattod.2014.04.026>
- [20] Lu, J., Chen, Q., Chen, S., Jiang, H., Liu, Y., & Chen, R. (2020). Pd Nanoparticles Loaded on Ceramic Membranes by Atomic Layer Deposition with Enhanced Catalytic Properties. *Industrial & Engineering Chemistry Research*, 59(44), 19564–19573. <https://doi.org/10.1021/acs.iecr.0c04158>
- [21] Fu, M., Wang, J., Heijman, B., & Van der Hoek, J. P. (2021). Removal of organic micropollutants by well-tailored granular zeolites and subsequent ozone-based regeneration. *Journal of Water Process Engineering*, 44, 102403. <https://doi.org/10.1016/j.jwpe.2021.102403>
- [22] Zhang, S., Sun, M., Hedtke, T., Deshmukh, A., Zhou, X., Weon, S., Elimelech, M., & Kim, J.-H. (2020). Mechanism of Heterogeneous Fenton Reaction Kinetics Enhancement under Nanoscale Spatial Confinement. *Environmental Science & Technology*, 54(17), 10868–10875. <https://doi.org/10.1021/acs.est.0c02192>
- [23] Luiza, K., Oliander. (2022). Food additives as environmental micropollutants. doi: 10.1016/b978-0-323-90555-8.00013-1
- [24] Eregowda, T., & Mohapatra, S. (2020). *Fate of Micropollutants in Engineered and Natural Environment. Resilience, Response, and Risk in Water Systems* (pp. 283–301). Springer Singapore. doi:

10.1007/978-981-15-4668-6\_15

- [25] Wang, S., Wasswa, J., Feldman, A. C., Kabenge, I., Kiggundu, N., & Zeng, T. (2022). Suspect screening to support source identification and risk assessment of organic micropollutants in the aquatic environment of a Sub-Saharan African urban center. *Water Research*, 220, 118706. <https://doi.org/10.1016/j.watres.2022.118706>
- [26] G., Raszewski., Konrad, Jamka., H., Bojar., Grzegorz, Kania. (2022). Endocrine disrupting micropollutants in water and their effects on human fertility and fecundity. *Annals of Agricultural and Environmental Medicine*, doi: 10.26444/aaem/156694
- [27] Khoo, Y. S., Goh, P. S., Lau, W. J., Ismail, A. F., Abdullah, M. S., Mohd Ghazali, N. H., Yahaya, N. K. E., Hashim, N., Othman, A. R., Mohammed, A., Kerisnan, N. D. A., Mohamed Yusoff, M. A., Fazlin Hashim, N. H., Karim, J., & Abdullah, N. S. (2022). Removal of emerging organic micropollutants via modified-reverse osmosis/nanofiltration membranes: A review. *Chemosphere*, 305, 135151. <https://doi.org/10.1016/j.chemosphere.2022.135151>
- [28] Tagliavini, M., Engel, F., Weidler, P. G., Scherer, T., & Schäfer, A. I. (2017). Adsorption of steroid micropollutants on polymer-based spherical activated carbon (PBSAC). *Journal of Hazardous Materials*, 337, 126-137. <https://doi.org/10.1016/j.jhazmat.2017.03.036>
- [29] Castaño Osorio, S., Biesheuvel, P., Spruijt, E., Dykstra, J., & Van der Wal, A. (2022). Modeling micropollutant removal by nanofiltration and reverse osmosis membranes: Considerations and challenges. *Water Research*, 225, 119130. <https://doi.org/10.1016/j.watres.2022.119130>
- [30] Mänttari, M., Pihlajamäki, A., & Nyström, M. (2006). Effect of pH on hydrophilicity and charge and their effect on the filtration efficiency of NF membranes at different pH. *Journal of Membrane Science*, 280(1-2), 311-320. <https://doi.org/10.1016/j.memsci.2006.01.034>
- [31] Luo, J., & Wan, Y. (2013). Effects of pH and salt on nanofiltration—A critical review. *Journal of Membrane Science*, 438, 18-28. <https://doi.org/10.1016/j.memsci.2013.03.029>
- [32] Fernández, R. L., McDonald, J. A., Khan, S. J., & Le-Clech, P. (2014). Removal of pharmaceuticals and endocrine disrupting chemicals by a submerged membrane photocatalysis reactor (MPR). *Separation and Purification Technology*, 127, 131-139. <https://doi.org/10.1016/j.seppur.2014.02.031>
- [33] Golovko, O., Rehrl, A., Köhler, S., & Ahrens, L. (2020). Organic micropollutants in water and sediment from Lake Mälaren, Sweden. *Chemosphere*, 258, 127293. <https://doi.org/10.1016/j.chemosphere.2020.127293>
- [34] Yoon, Y., Westerhoff, P., Snyder, S. A., Wert, E. C., & Yoon, J. (2007). Removal of endocrine disrupting compounds and pharmaceuticals by nanofiltration and ultrafiltration membranes. *Desalination*, 202(1-3), 16-23. <https://doi.org/10.1016/j.desal.2005.12.033>
- [35] Nunes, S.P. (2022). Polymeric Membranes. In *Macromolecular Engineering* (eds N. Hadjichristidis, Y. Gnanou, K. Matyjaszewski and M. Muthukumar). <https://doi.org/10.1002/9783527815562.mme0048>
- [36] Sharma, S., Gupta, S., Kaur, S., Kumar, D., Banerjee, P., Nadda, A.K. (2023). Polymeric Membranes for Water Treatment. In: Nadda, A.K., Banerjee, P., Sharma, S., Nguyen-Tri, P. (eds) *Membranes for Water Treatment and Remediation. Materials Horizons: From Nature to Nanomaterials*. Springer, Singapore. [https://doi.org/10.1007/978-981-19-9176-9\\_1](https://doi.org/10.1007/978-981-19-9176-9_1)

- [37] Sonawane, S., Thakur, P., Sonawane, S. H., & Bhanvase, B. A. (2020). Nanomaterials for membrane synthesis: Introduction, mechanism, and challenges for wastewater treatment. *Handbook of Nanomaterials for Wastewater Treatment*, 537-553. <https://doi.org/10.1016/B978-0-12-821496-1.00009-X>
- [38] De Napoli, I., Catapano, G., Ebrahimi, M., & Czermak, P. (2010). Novel and Current Techniques to Produce Endotoxin-Free Dialysate in Dialysis Centers. *Comprehensive Biotechnology (Second Edition)*, 741-752. <https://doi.org/10.1016/B978-0-08-088504-9.00516-X>
- [39] Shi, X., Tal, G., Hankins, N. P., & Gitis, V. (2014). Fouling and cleaning of ultrafiltration membranes: A review. *Journal of Water Process Engineering*, 1, 121-138. <https://doi.org/10.1016/j.jwpe.2014.04.003>
- [40] Alkhatib, A., Ayari, M. A., & Hawari, A. H. (2021). Fouling mitigation strategies for different foulants in membrane distillation. *Chemical Engineering and Processing - Process Intensification*, 167, 108517. <https://doi.org/10.1016/j.cep.2021.108517>
- [41] Ahmad, A. L., Che Lah, N. F., Ismail, S., & Ooi, B. S. (2012). Membrane Antifouling Methods and Alternatives: Ultrasound Approach. *Separation & Purification Reviews*, 41(4), 318–346. <https://doi.org/10.1080/15422119.2011.617804>
- [42] Gryta, M. (2007). Influence of polypropylene membrane surface porosity on the performance of membrane distillation process. *Journal of Membrane Science*, 287(1), 67-78. <https://doi.org/10.1016/j.memsci.2006.10.011>
- [43] Miklos, D. B., Remy, C., Jekel, M., Linden, K. G., Drewes, J. E., & Hübner, U. (2018). Evaluation of advanced oxidation processes for water and wastewater treatment – A critical review. *Water Research*, 139, 118-131. <https://doi.org/10.1016/j.watres.2018.03.042>
- [44] Neyens, E., & Baeyens, J. (2003). A review of classic Fenton's peroxidation as an advanced oxidation technique. *Journal of hazardous materials*, 98(1–3), 33–50. Netherlands.
- [45] Khan, M. (2022). Fenton, photo-Fenton, electro-Fenton, and their combined treatments for the removal of insecticides from waters and soils. A review. *Separation and Purification Technology*, doi: 10.1016/j.seppur.2021.120290
- [46] Sun, A., Zhao, H., Wang, M., Ma, J., Jin, H., & Zhang, K. (2022). One-Pot Synthesis of Pyrite Nanoplates Supported on Chitosan Hydrochar as Fenton Catalysts for Organics Removal from Water. *Catalysts*, 12(8), 858. <https://doi.org/10.3390/catal12080858>
- [47] Kolthoff, I. M., & Miller, I. K. (1951). The Chemistry of Persulfate. I. The Kinetics and Mechanism of the Decomposition of the Persulfate Ion in Aqueous Medium<sup>1</sup>. *Journal of the American Chemical Society*, 73(7), 3055–3059. <https://doi.org/10.1021/ja01151a024>
- [48] Zhang, X., Yao, J., Zhao, Z., & Liu, J. (2019). Degradation of haloacetonitriles with UV/peroxymonosulfate process: Degradation pathway and the role of hydroxyl radicals. *Chemical Engineering Journal*, 364, 1-10. <https://doi.org/10.1016/j.cej.2019.01.029>
- [49] Lin, Z., Qin, W., Sun, L., Yuan, X., & Xia, D. (2020). Kinetics and mechanism of sulfate radical- and hydroxyl radical-induced degradation of Bisphenol A in VUV/UV/peroxymonosulfate system. *Journal of Water Process Engineering*, 38, 101636. <https://doi.org/10.1016/j.jwpe.2020.101636>

- [50] Yang, Y., Jiang, J., Lu, X., Ma, J., & Liu, Y. (2015). Production of sulfate radical and hydroxyl radical by reaction of ozone with peroxydisulfate: a novel advanced oxidation process. *Environmental science & technology*, 49(12), 7330–9. <https://doi.org/10.1021/es506362e>
- [51] Liang, C., & Su, H.-W. (2009). Identification of Sulfate and Hydroxyl Radicals in Thermally Activated Persulfate. *Industrial & Engineering Chemistry Research*, 48(11), 5558–5562. <http://dx.doi.org/10.1021/ie9002848>
- [52] Ushani, U., Lu, X., Wang, J., Zhang, Z., Dai, J., Tan, Y., Wang, S., et al. (2020). Sulfate radicals-based advanced oxidation technology in various environmental remediation: A state-of-the-art review. *Chemical Engineering Journal*, 402, 126232. <https://doi.org/10.1016/j.cej.2020.126232>
- [53] Zhou, X., Zhao, Q., Wang, J., Chen, Z., & Chen, Z. (2021). Nonradical oxidation processes in PMS-based heterogeneous catalytic system: Generation, identification, oxidation characteristics, challenges response and application prospects. *Chemical Engineering Journal*, 410, 128312. <https://doi.org/10.1016/j.cej.2020.128312>
- [54] M Nie, M., Deng, Y., Nie, S., Yan, C., Ding, M., Dong, W., Dai, Y., & Zhang, Y. (2019). Simultaneous removal of bisphenol A and phosphate from water by peroxydisulfate combined with calcium hydroxide. *Chemical Engineering Journal*, 369, 35-45. <https://doi.org/10.1016/j.cej.2019.03.046>
- [55] Li, Z., Sun, Y., Yang, Y., Han, Y., Wang, T., Chen, J., & Tsang, D. C. (2020). Biochar-supported nanoscale zero-valent iron as an efficient catalyst for organic degradation in groundwater. *Journal of Hazardous Materials*, 383, 121240. <https://doi.org/10.1016/j.jhazmat.2019.121240>
- [56] Li, H., Shan, C., Li, W., & Pan, B. (2018). Peroxydisulfate activation by iron(III)-tetraamidomacrocyclic ligand for degradation of organic pollutants via high-valent iron-oxo complex. *Water Research*, 147, 233-241. <https://doi.org/10.1016/j.watres.2018.10.015>
- [57] Wang, L., Xiao, K., & Zhao, H. (2023). The debatable role of singlet oxygen in persulfate-based advanced oxidation processes. *Water Research*, 235, 119925. <https://doi.org/10.1016/j.watres.2023.119925>
- [58] Bennedsen, L. R., Muff, J., & Søgaard, E. G. (2012). Influence of chloride and carbonates on the reactivity of activated persulfate. *Chemosphere*, 86(11), 1092-1097. <https://doi.org/10.1016/j.chemosphere.2011.12.011>
- [59] Chan, K., & Chu, W. (2009). Degradation of atrazine by cobalt-mediated activation of peroxydisulfate: Different cobalt counteranions in homogenous process and cobalt oxide catalysts in photolytic heterogeneous process. *Water Research*, 43(9), 2513-2521. <https://doi.org/10.1016/j.watres.2009.02.029>
- [60] Lin, Z., Qin, W., Sun, L., Yuan, X., & Xia, D. (2020). Kinetics and mechanism of sulfate radical- and hydroxyl radical-induced degradation of Bisphenol A in VUV/UV/p peroxydisulfate system. *Journal of Water Process Engineering*, 38, 101636. <https://doi.org/10.1016/j.jwpe.2020.101636>
- [61] Wang, Z., Yuan, R., Guo, Y., Xu, L., & Liu, J. (2011). Effects of chloride ions on bleaching of azo dyes by Co<sup>2+</sup>/oxone reagent: Kinetic analysis. *Journal of Hazardous Materials*, 190(1-3), 1083-1087. <https://doi.org/10.1016/j.jhazmat.2011.04.016>

- [62] Ji, Y., Dong, C., Kong, D., & Lu, J. (2015). New insights into atrazine degradation by cobalt catalyzed peroxymonosulfate oxidation: Kinetics, reaction products and transformation mechanisms. *Journal of Hazardous Materials*, 285, 491-500. <https://doi.org/10.1016/j.jhazmat.2014.12.026>
- [63] Yao, Y., Chen, H., Qin, J., Wu, G., Lian, C., Zhang, J., & Wang, S. (2016). Iron encapsulated in boron and nitrogen codoped carbon nanotubes as synergistic catalysts for Fenton-like reaction. *Water Research*, 101, 281-291. <https://doi.org/10.1016/j.watres.2016.05.065>
- [64] Weishaar, J. L., Aiken, G. R., Bergamaschi, B. A., Fram, M. S., Fujii, R., & Mopper, K. (2003). Evaluation of specific ultraviolet absorbance as an indicator of the chemical composition and reactivity of dissolved organic carbon. *Environmental science & technology*, 37(20), 4702-8. <https://doi.org/10.1021/es030360x>
- [65] Bolto, B., Dixon, D., Eldridge, R., King, S., & Linge, K. (2002). Removal of natural organic matter by ion exchange. *Water Research*, 36(20), 5057-5065. [https://doi.org/10.1016/S0043-1354\(02\)00231-2](https://doi.org/10.1016/S0043-1354(02)00231-2)
- [66] Mansas, C., Mendret, J., Brosillon, S., & Ayrat, A. (2020). Coupling catalytic ozonation and membrane separation: A review. *Separation and Purification Technology*, 236, 116221. <https://doi.org/10.1016/j.seppur.2019.116221>
- [67] Hög, A., Ludwig, J., & Beery, M. (2015). The use of integrated flotation and ceramic membrane filtration for surface water treatment with high loads of suspended and dissolved organic matter. *Journal of Water Process Engineering*, 6, 129-135. <https://doi.org/10.1016/j.jwpe.2015.03.010>
- [68] Álvarez, P., Beltrán, F., Pocostales, J., & Masa, F. (2007). Preparation and structural characterization of Co/Al<sub>2</sub>O<sub>3</sub> catalysts for the ozonation of pyruvic acid. *Applied Catalysis B: Environmental*, 72(3-4), 322-330. <https://doi.org/10.1016/j.apcatb.2006.11.009>
- [69] Park, H., Kim, Y., An, B., & Choi, H. (2012). Characterization of natural organic matter treated by iron oxide nanoparticle incorporated ceramic membrane-ozonation process. *Water Research*, 46(18), 5861-5870. <https://doi.org/10.1016/j.watres.2012.07.039>
- [70] Luo, X., Yu, S., Xu, D., Ding, J., Zhu, X., Xing, J., Wu, T., Zheng, X., Aminabhavi, T. M., Cheng, X., & Liang, H. (2022). Isoporous catalytic ceramic membranes for ultrafast contaminants elimination through boosting confined radicals. *Chemical Engineering Journal*, 455, 140872. <https://doi.org/10.1016/j.cej.2022.140872>
- [71] Demirtaş, M., Odacı, C., Shehu, Y., Perkgöz, N. K., & Ay, F. (2020). Layer and size distribution control of CVD-grown 2D MoS<sub>2</sub> using ALD-deposited MoO<sub>3</sub> structures as the precursor. *Materials Science in Semiconductor Processing*, 108, 104880. <https://doi.org/10.1016/j.mssp.2019.104880>
- [72] Fraga, M., & Pessoa, R. (2020). Progresses in Synthesis and Application of SiC Films: From CVD to ALD and from MEMS to NEMS. *Micromachines*, 11(9), 799. <https://doi.org/10.3390/mi11090799>
- [73] Elam, J. W., Zinovev, A., Han, C. Y., Wang, H. H., Welp, U., Hryn, J. N., & Pellin, M. J. (2006). Atomic layer deposition of palladium films on Al<sub>2</sub>O<sub>3</sub> surfaces. *Thin Solid Films*, 515(4), 1664-1673. <https://doi.org/10.1016/j.tsf.2006.05.049>
- [74] Liang, C., Huang, C., Mohanty, N., & Kurakalva, R. M. (2008). A rapid spectrophotometric determination of persulfate anion in ISCO. *Chemosphere*, 73(9), 1540-1543. <https://doi.org/10.1016/j.chemosphere.2008.08.043>

- [75] Khan, S., Han, C., Sayed, M., Sohail, M., Jan, S., Sultana, S., Khan, H. M., & Dionysiou, D. D. (2019). Exhaustive photocatalytic lindane degradation by combined simulated solar light-activated nanocrystalline TiO<sub>2</sub> and inorganic oxidants. *Catalysts*, 9(5). <https://doi.org/10.3390/catal9050425>
- [76] Ma, M., Chen, L., Zhao, J., Liu, W., & Ji, H. (2019). Efficient activation of peroxymonosulfate by hollow cobalt hydroxide for degradation of ibuprofen and theoretical study. *Chinese Chemical Letters*, 30(12), 2191–2195. <https://doi.org/https://doi.org/10.1016/j.ccllet.2019.09.031>
- [77] Liu, W., Li, Y., Liu, F., Jiang, W., Zhang, D., & Liang, J. (2019). Visible-light-driven photocatalytic degradation of diclofenac by carbon quantum dots modified porous g-C<sub>3</sub>N<sub>4</sub>: Mechanisms, degradation pathway and DFT calculation. *Water Research*, 151, 8–19. <https://doi.org/https://doi.org/10.1016/j.watres.2018.11.084>
- [78] Guo, Y., Long, J., Huang, J., Yu, G., & Wang, Y. (2022). Can the commonly used quenching method really evaluate the role of reactive oxygen species in pollutant abatement during catalytic ozonation? *Water Research*, 215, 118275. <https://doi.org/10.1016/j.watres.2022.118275>
- [79] Xiao, R., Fu, Y., Bai, L., Chu, C., Ma, J., Wei, Z., Spinney, R., Dionysiou, D. D., & Pu, J. (2022). Kinetics and mechanistic aspects of superoxide radical-mediated transformation of ascorbate. *Journal of Environmental Chemical Engineering*, 10(3), 107736. <https://doi.org/10.1016/j.jece.2022.107736>
- [80] Yu, Y., Li, H., Chen, J., Wang, F., Chen, X., Huang, B., He, Y., & Cai, Z. (2022). Exploring the adsorption behavior of benzotriazoles and benzothiazoles on polyvinyl chloride microplastics in the water environment. *Science of The Total Environment*, 821, 153471. <https://doi.org/10.1016/j.scitotenv.2022.153471>
- [81] Tseng, L. Y., You, C., Vu, C., Chistolini, M. K., Wang, C. Y., Mast, K., Luo, F., et al. (2022). Adsorption of Contaminants of Emerging Concern (CECs) with Varying Hydrophobicity on Macro- and Microplastic Polyvinyl Chloride, Polyethylene, and Polystyrene: Kinetics and Potential Mechanisms. <https://doi.org/10.3390/w14162581>
- [82] M. Mohamed, M. S., Asair, A. A., H. Fetyan, N. A., & Elnagdy, S. M. (2023). Complete Biodegradation of Diclofenac by New Bacterial Strains: Postulated Pathways and Degrading Enzymes. *Microorganisms*, 11(6). <https://doi.org/10.3390/microorganisms11061445>
- [83] Liu, T., Zhang, D., Yin, K., Yang, C., Luo, S., & Crittenden, J. C. (2020). Degradation of thiacloprid via unactivated peroxymonosulfate: The overlooked singlet oxygen oxidation. *Chemical Engineering Journal*, 388, 124264. <https://doi.org/10.1016/j.cej.2020.124264>
- [84] Ji, Y., Lu, J., Wang, L., Jiang, M., Yang, Y., Yang, P., Zhou, L., Ferronato, C., & Chovelon, J. (2018). Non-activated peroxymonosulfate oxidation of sulfonamide antibiotics in water: Kinetics, mechanisms, and implications for water treatment. *Water Research*, 147, 82-90. <https://doi.org/10.1016/j.watres.2018.09.037>
- [85] Huang, Y., Guan, Z., Li, Q., Li, Q., & Xia, D. (2023). Preparation, performance and mechanism of metal oxide modified catalytic ceramic membranes for wastewater treatment. *RSC advances*, 13(25), 17436–17448. <https://doi.org/10.1039/D3RA01291C>
- [86] Maruthamuthu, P., & Neta, P. (1977). Radiolytic chain decomposition of peroxomonophosphoric and peroxomonosulfuric acids. *The Journal of Physical Chemistry*, 81(10), 937–940. <https://doi.org/10.1021/j100525a001>

- [87] Liu, Y., He, X., Fu, Y., & Dionysiou, D. D. (2016). Kinetics and mechanism investigation on the destruction of oxytetracycline by UV-254 nm activation of persulfate. *Journal of Hazardous Materials*, 305, 229-239. <https://doi.org/10.1016/j.jhazmat.2015.11.043>
- [88] Rastogi, A., Al-Abed, S. R., & Dionysiou, D. D. (2009). Sulfate radical-based ferrous–peroxymonosulfate oxidative system for PCBs degradation in aqueous and sediment systems. *Applied Catalysis B: Environmental*, 85(3-4), 171-179. <https://doi.org/10.1016/j.apcatb.2008.07.010>
- [89] Liu, Y., He, X., Duan, X., Fu, Y., & Dionysiou, D. D. (2015). Photochemical degradation of oxytetracycline: Influence of pH and role of carbonate radical. *Chemical Engineering Journal*, 276, 113-121. <https://doi.org/10.1016/j.cej.2015.04.048>
- [90] Ball, D. L., & Edwards, J. O. (1956). The Kinetics and Mechanism of the Decomposition of Caro's Acid. I. *Journal of the American Chemical Society*, 78(6), 1125–1129. <https://doi.org/10.1021/ja01587a011>
- [91] Lente, G., Kalmár, J., Baranyai, Z., Kun, A., Kék, I., Bajusz, D., Takács, M., et al. (2009). One-Versus Two-Electron Oxidation with Peroxomonosulfate Ion: Reactions with Iron(II), Vanadium(IV), Halide Ions, and Photoreaction with Cerium(III). *Inorganic Chemistry*, 48(4), 1763–1773. <https://doi.org/10.1021/ic801569k>
- [92] Zhao, W., Duan, Z., Zheng, Z., & Li, B. (2022). Efficient diclofenac removal by superoxide radical and singlet oxygen generated in surface Mn(II)/(III)/(IV) cycle dominated peroxymonosulfate activation system: Mechanism and product toxicity. *Chemical Engineering Journal*, 433, 133742. <https://doi.org/10.1016/j.cej.2021.133742>
- [93] Liu, Y., Guo, H., Zhang, Y., Cheng, X., Zhou, P., Deng, J., Wang, J., & Li, W. (2019). Highly efficient removal of trimethoprim based on peroxymonosulfate activation by carbonized resin with Co doping: Performance, mechanism and degradation pathway. *Chemical Engineering Journal*, 356, 717-726. <https://doi.org/10.1016/j.cej.2018.09.086>
- [94] Ghanbari, F., Khatebasreh, M., Mahdavianpour, M., & Lin, K. A. (2020). Oxidative removal of benzotriazole using peroxymonosulfate/ozone/ultrasound: Synergy, optimization, degradation intermediates and utilizing for real wastewater. *Chemosphere*, 244, 125326. <https://doi.org/10.1016/j.chemosphere.2019.125326>
- [95] Jorfi, S., Kakavandi, B., Motlagh, H. R., Ahmadi, M., & Jaafarzadeh, N. (2017). A novel combination of oxidative degradation for benzotriazole removal using TiO<sub>2</sub> loaded on FeII/FeIII/Fe<sub>2</sub>O<sub>4</sub>@C as an efficient activator of peroxymonosulfate. *Applied Catalysis B: Environmental*, 219, 216-230. <https://doi.org/10.1016/j.apcatb.2017.07.035>
- [96] Senila, M., Cadar, O., Senila, L., Böringer, S., Seaudeau-Pirouley, K., Ruiu, A., & Lacroix-Desmazes, P. (2020). Performance Parameters of Inductively Coupled Plasma Optical Emission Spectrometry and Graphite Furnace Atomic Absorption Spectrometry Techniques for Pd and Pt Determination in Automotive Catalysts. *Materials*, 13(22). <https://doi.org/10.3390/ma13225136>

## 8 Appendix

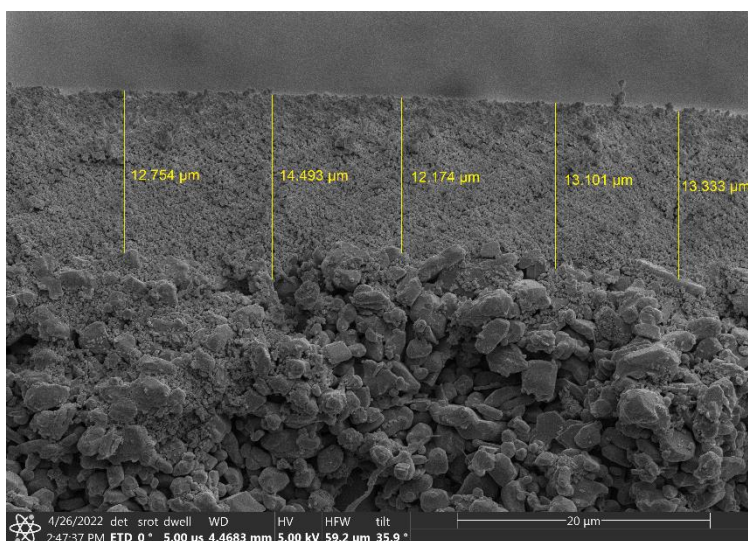


**Figure S 1:** SEM image of the filtration layer of 60-cycle membrane, measured by ImageJ

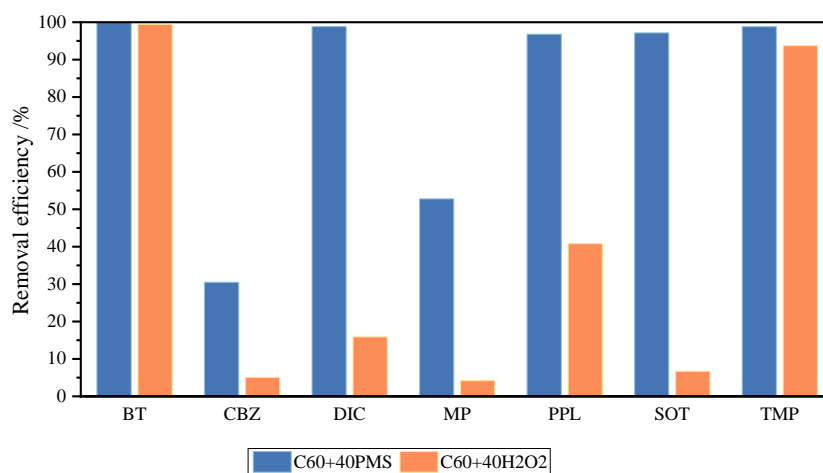


**Figure S 2:** Comparison of the average removal efficiencies of OMPs within 50 minutes for 60-cycle membrane (C60) with the addition of 40 $\mu$ M PMS, and with 40 $\mu$ M H<sub>2</sub>O<sub>2</sub>.

Default condition: pH = 7, flux = 30 LMH.

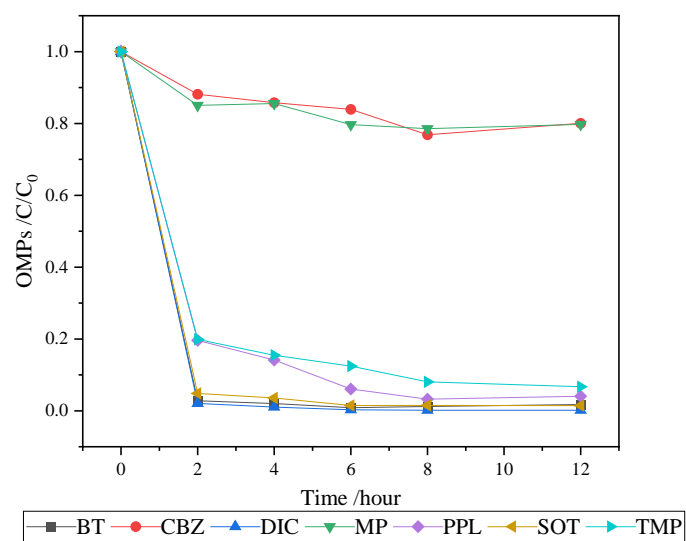


**Figure S 3:** Changes of OMPs residual ratio over 12-hour test

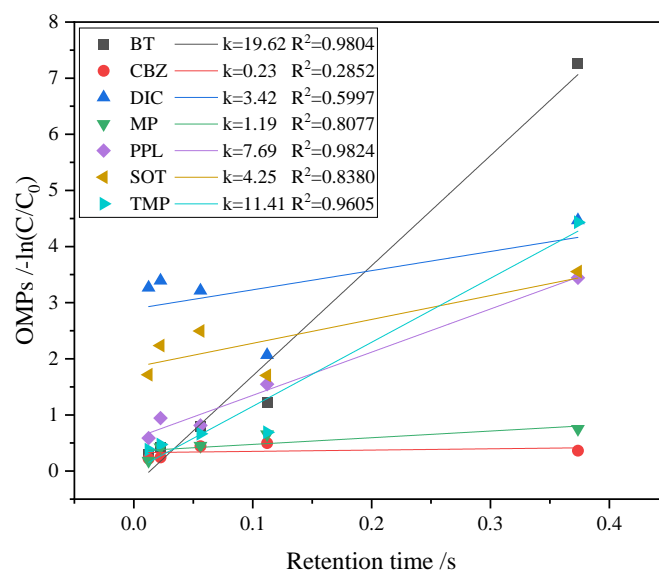
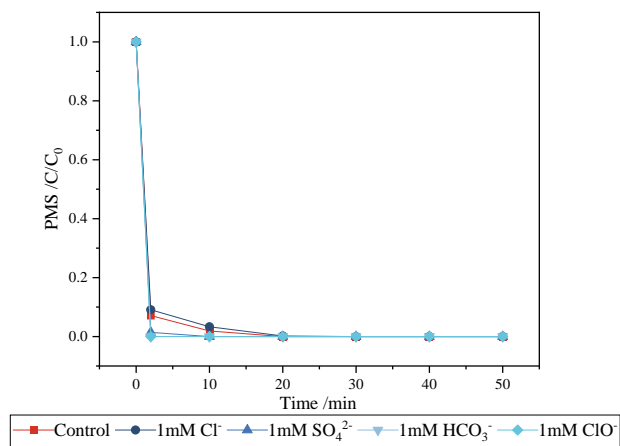
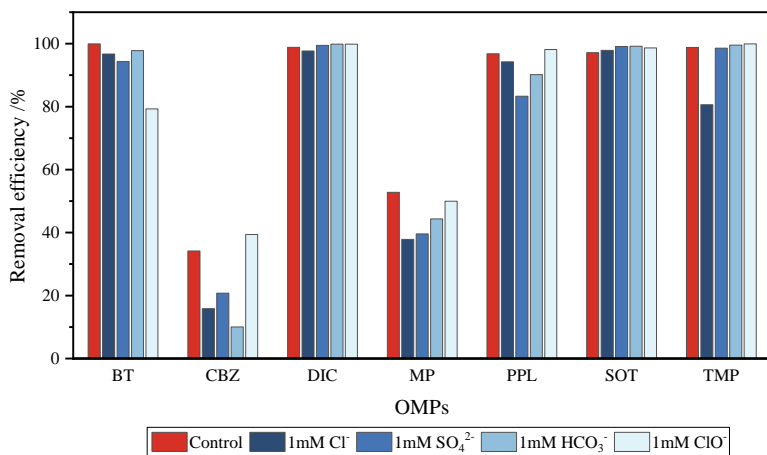


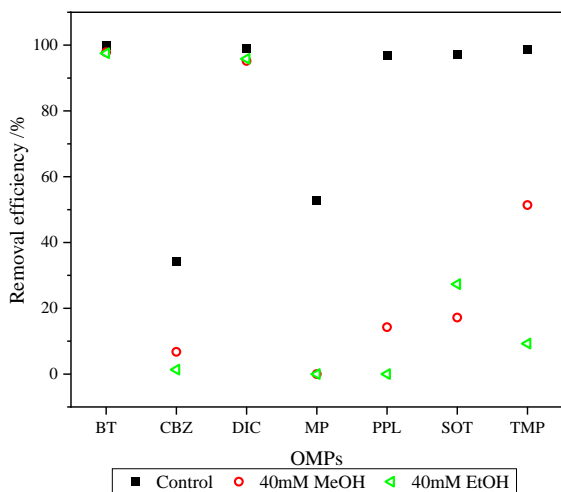
**Figure S 4:** The reaction rate of various OMPs, fitted with pseudo-first-order kinetics



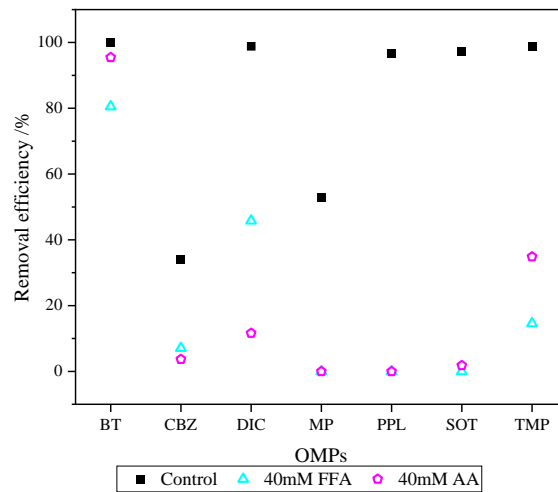
a

b

**Figure S 5:** (a) The removal efficiency of OMPs in the presence of 1 mM Cl<sup>-</sup>, 1 mM SO<sub>4</sub><sup>2-</sup>, 1 mM HCO<sub>3</sub><sup>-</sup>, 1 mM ClO<sup>-</sup> and without any ions (control group); (b) PMS residual concentration ratio (C/C<sub>0</sub>) under corresponding conditions.



a



b

**Figure S 6:** (a) Removal efficiency of OMPs in the absence of scavenger (control) and with 40 mM of methanol (quench <sup>•</sup>OH, SO<sub>4</sub><sup>-</sup>), ethanol (<sup>•</sup>OH, SO<sub>4</sub><sup>-</sup>); (b) OMPs removal efficiency in the control group and with 0.4 mM of furfuryl alcohol (<sup>1</sup>O<sub>2</sub>); and L-ascorbic acid (O<sub>2</sub><sup>-</sup>); Experiments condition: 30 LMH of flux, 40 μm PMS, pH 7

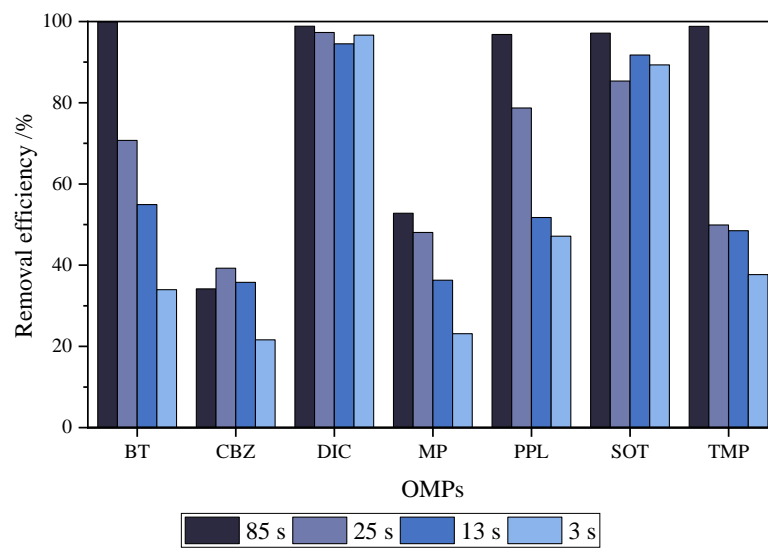


**Figure S 7:** Removal efficiency of OMPs by both the pores and surface catalysis. (Experiments condition: pH=7, 40 $\mu$ m PMS, retention time= 3, 13, 26, 85s)

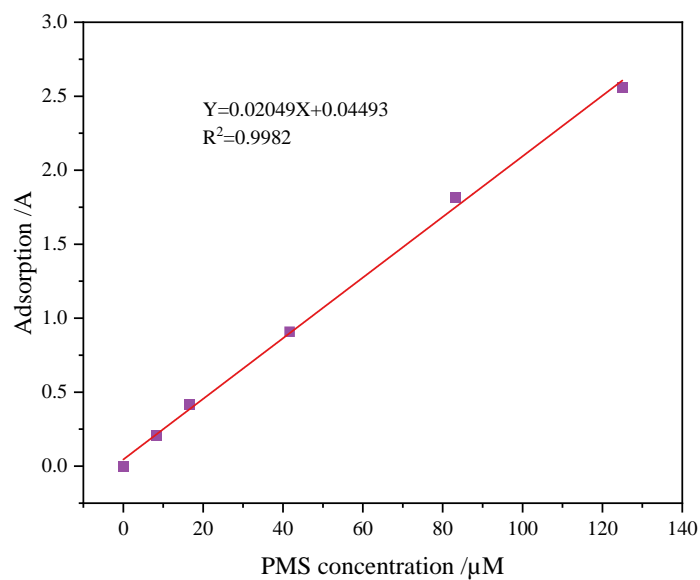


**Figure S 8:** The calibration line of PMS

**Table 6: Calculation of retention time (Eq.(13))**

Flux (L/m <sup>2</sup> /h)	Porosity (%)	Filtration layer thickness (m)	Retention time (s)
30	23.63	$1.3171 \times 10^{-5}$	0.3736
100			0.1121
200			0.0560
500			0.0224
900			0.0125